Geologic Hazards, Earthquake and Landslide Hazard Maps, and Future Earthquake Damage Estimates

for Six Counties in the Mid/Southern Willamette Valley Including Yamhill, Marion, Polk, Benton, Linn, and Lane Counties, and the City of Albany, Oregon

by William J. Burns, R. Jon Hofmeister, and Yumei Wang

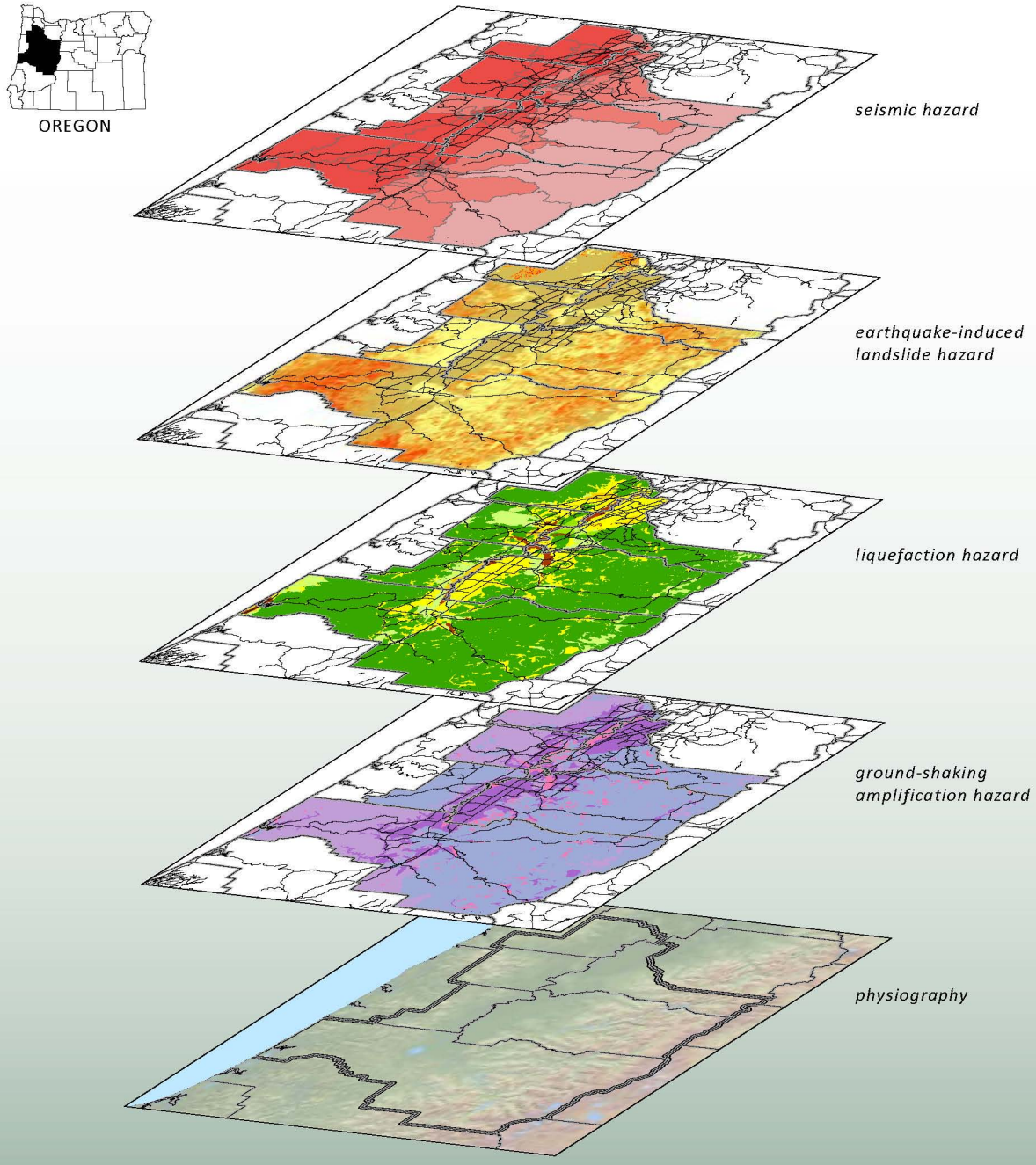

OREGON DEPARTMENT OF GEOLOGY AND MINERAL INDUSTRIES INTERPRETIVE MAP SERIES IMS-24

Cover: Map layers (from bottom to top) are from maps shown in Figures 2, 16, 17, and 19 in the main text and a composite of Figure 4 from appendices A–G.

State of Oregon
Department of Geology and Mineral Industries
Vicki S. McConnell, State Geologist

Interpretive Map Series
IMS-24

GEOLOGIC HAZARDS, EARTHQUAKE AND LANDSLIDE HAZARD MAPS, AND FUTURE EARTHQUAKE DAMAGE ESTIMATES FOR SIX COUNTIES IN THE MID/SOUTHERN WILLAMETTE VALLEY INCLUDING YAMHILL, MARION, POLK, BENTON, LINN, AND LANE COUNTIES, AND THE CITY OF ALBANY, OREGON

By
William J. Burns[1], R. Jon Hofmeister[2], and Yumei Wang[1]

2008

[1]Oregon Department of Geology and Mineral Industries, 800 NE Oregon Street #28, Suite 965, Portland, Oregon 97232
[2]Formerly with Oregon Department of Geology and Mineral Industries

DISCLAIMER

Maps in this publication depict relative earthquake and landslide hazard zones on the basis of limited data as described further in the text. The maps cannot serve as a substitute for site-specific investigations by qualified practitioners. Site-specific data may give results that differ from those shown on the maps. The maps can be used as a general guide for emergency response planning.

Oregon Department of Geology and Mineral Industries Interpretive Map Series IMS-24
Published in conformance with ORS 516.030

For copies of this publication or other information about Oregon's geology and natural resources, contact:

Nature of the Northwest Information Center
800 NE Oregon Street #5, Suite 177
Portland, Oregon 97232
(503) 872-2750
http://www.naturenw.org

or these DOGAMI field offices:

Baker City Field Office
1510 Campbell St.
Baker City, OR 97814-3442
Telephone (541) 523-3133
Fax (541) 523-5992

Grants Pass Field Office
5375 Monument Drive
Grants Pass, OR 97526
Telephone (541) 476-2496
Fax (541) 474-3158

For additional information:
Administrative Offices
800 NE Oregon Street #28, Suite 965
Portland, OR 97232
Telephone (971) 673-1555
Fax (971) 673-1562
http://www.oregongeology.com
http://egov.oregon.gov/DOGAMI/

TABLE OF CONTENTS

APPENDICES

LIST OF FIGURES

(continued on next page)

List of Figures, continued

(continued on next page)

List of Figures, continued

LIST OF TABLES

LIST OF PLATES

1.0 EXECUTIVE SUMMARY

To become resilient from geologic hazards, communities in Oregon have begun a large-scale endeavor to perform pre-disaster mitigation. A first step in this process is the development of natural hazards mitigation plans. For this project, six counties and one city in the Mid/Southern Willamette Valley (Oregon Partnership for Disaster Resilience Region 3) merged together resources to begin:

- Identifying potential natural hazards
- Identifying vulnerability to these hazards
- Assessing the level of risk, and thus
- Increasing the level of resilience through pre-disaster mitigation

To assist planners in the developing their natural hazards mitigation plans, the Department of Geology and Mineral Industries (DOGAMI) performed the following tasks related to geologic hazards:

- Identified the primary geologic hazards of Yamhill, Marion, Polk, Benton, Linn, and Lane Counties and the City of Albany (herein known as the study area or individual communities)
- Developed countywide earthquake and landslide hazard maps for each county
- Developed future earthquake damage estimates for each community

The purpose of this study is to help communities prepare pre-disaster mitigation plans, to identify potential geologic hazards, to help communities perform earthquake damage and loss estimation, and to recommend future action items. Several products have been generated as part of this project. They include digital geographic information system (GIS) layers for each community, depicting:

- Relative earthquake ground-shaking amplification hazards
- Relative earthquake liquefaction hazards
- Relative earthquake-induced landslide hazards
- Identified landslide areas

Damage and loss estimates for each community were analyzed for two earthquake scenarios:

- A magnitude ~6.5 crustal fault earthquake
- A magnitude 9.0 Cascadia Subduction Zone earthquake

To improve existing hazard maps and data, action items are provided. These action items range from site-specific items such as identification of individual school buildings that have a high risk of collapse in an earthquake to identification of landslide hazard areas over large regions of the state.

Identified earthquake-induced hazards include ground-shaking amplification, liquefaction, earthquake-induced landslides, and tsunamis. To evaluate non-earthquake related landslide hazards, we used identified landslide areas, potential "rapidly moving landslide" (debris flow) hazards maps, and an inventory of slope failures in Oregon from three storm events (1996-1997). Dam failures are frequently caused by geologic hazard events, and we evaluate these. Finally, we discuss volcanic hazards from Mount Jefferson and the Three Sisters region.

The relative earthquake hazard maps developed in this study identify areas of higher or lower potential hazard and can help guide planners who must determine which areas should require future site-specific seismic evaluations. The identified landslide areas map is a digitized compilation of previously identified landslides. All of these maps should only serve as a guide for future site-specific evaluations.

Ground-shaking amplification and liquefaction hazards are usually highest in the young, soft alluvial sediments of the Willamette Valley and along other major stream channels. Landslide hazards are highest in steep, mountainous terrain and at the base of steep canyons. Landslide areas identified in the accompanying GIS files also pose significant hazards for development.

We used regional earthquake hazard information developed in this study to assess potential damage and loss for various earthquake scenarios. We consolidated information into the Hazards U.S. Multi-Hazard methodology and computer application (HAZUS-MH), which is a federally developed program used to model various earthquake scenarios and estimate associated damage and loss. With the improved HAZUS-MH study regions (included with this report), we modeled damage and loss estimates for two earthquake scenarios — resulting in expected total building damage on the order of $11.7 billion for a Cascadia Subduction Zone event.

The products from this study can be used to help mid/southern Willamette Valley communities become more resilient from the impacts of geologic hazards through pre-disaster mitigation.

2.0 INTRODUCTION

The three main objectives of this study were 1) to assist communities in development of county and city pre-disaster mitigation plans, 2) to identify and map potential geologic hazards and to improve the abilities of the communities to perform earthquake damage and loss estimation, and 3) to recommend future action items. The body of this report describes the results for these three objectives.

This study was initiated by the U.S. Department of Homeland Security's Federal Emergency Management Agency (FEMA) Pre-Disaster Mitigation (PDM) grant program, which provides funds to states, territories, Indian tribes, communities, colleges, and universities for pre-disaster mitigation planning efforts to better address natural hazards.

Geologic hazards pose a significant threat in many parts of Oregon. For example, earthquakes as large as magnitude 9.0 have occurred along the offshore Cascadia Subduction Zone repeatedly in the geologic past (Atwater, 1987; Yamaguchi and others, 1997), and the scientific consensus is that they will happen again (Clague and others, 2000). Smaller crustal earthquakes, which can be more damaging in local areas than subduction zone earthquakes, also pose significant risks where faults are close to urban areas. Important reminders of the dangers and effects of local earthquakes include the magnitude 5.6 earthquake that occurred near Scotts Mills, Oregon, in 1993 and the Klamath Falls, Oregon, earthquakes (magnitudes 5.9 and 6.0) that occurred later that year. Combined, these earthquakes caused more than $40 million in direct damage, and there were two fatalities in the Klamath Falls earthquakes (Wiley and others, 1993).

Many parts of Oregon are also highly susceptible to landslides. Landslides pose significant threats to people and infrastructure, particularly in the portions of the state with moderate to steep slopes. As population growth continues and as development into steeper terrain occurs, greater losses are likely to result. Most of Oregon's landslide damage has been associated with severe winter storms where landslide losses exceed $100 million in direct damage (such as the February 1996 event; see FEMA [1996]). Annual average maintenance and repair costs for landslides in Oregon are over $10 million (Wang and others, 2002). Landslides induced by earthquake shaking are likely in many parts of Oregon, and losses associated with sliding in moderate-to-large earthquakes are likely to be significant. Volcanic hazards and dam failure due to geologic hazards are also potential threats to many parts of Oregon.

3.0 PREVIOUS WORK

A number of previous regional and site-specific geologic and geologic hazard studies have been conducted throughout the study area to identify natural hazards, to assess risks, and to mitigate hazards. In our current efforts, we consolidate this large body of work into a GIS database to help assess hazards affecting the study area and we highlight some possible ways individual communities can address these hazards.

For the earthquake hazard mapping components of this study, we used a number of previously developed geologic maps and other related data. Specific sources of geologic information include Allison (1953), Allison and Felts (1956), Baldwin (1956, 1964, 1974), Beaulieu and others (1974), Bela (1981), Black and others (1987), Brown (1980), Brown and others (1980), Brownfield (1982a, 1982b, 1982c), Brownfield and Schlicker (1981a, 1981b), Hladky and McCaslin (2005), Madin and Murray (2003, 2005), Madin and others (2006), Miller and Orr (1984a, 1984b), Murray (2005), Niem and others (1989), O'Connor and others (2001), Orr and Miller (1984, 1986), Priest and others (1987, 1988), Ramp (1972), Schlicker (1967), Schlicker and others (1974), Sherrod (1988), Snavely and others (1976), Thayer (1939), Tolan and others (1999), Vokes and others (1951), Walker and Duncan (1989), Walker and others (2002), Wells and others (1983), and White (1980).

In addition to traditional geologic maps, natural hazard maps have been developed for portions of the counties. These include publications by Bela (1979), Black and others (2000), Burns and others (1997), Harvey and Peterson (1998, 2000), Hofmeister and others (2000), Hofmeister and Wang (2000), Madin and Wang (2000a, 2000b), Madin and Wang (1999), Madin and Wang (2000c), Schlicker and Deacon (1967), Wang and Leonard (1996), and Wang and others (2001). Appendix H includes list of these publications (Table H1) with reference numbers that are identified spatially in Figure H4.

For the earthquake damage and loss estimation portion of this study, we used information from several data sources and publications. A report specific to Benton County geologic hazards loss estimation was developed in 2001 (Wang and others, 2001). The report includes building inventory information, background discussion of natural hazards in the county, and initial loss estimations for earthquakes. Rogers and others (1998) provide overall reviews of earthquake hazards in the Pacific Northwest; Turner and Schuster (1996) summarize landslide types and characteristics; and Spangle Associates (1998) summarizes potential uses of natural hazard maps in Oregon.

4.0 STUDY AREA

The study covers an area of 26,520 km^2 (10,240 mi^2) and is geographically bounded by Chehalem Mountain to the north, the peaks of the Coast Range to the west (with the exception of Lane County, which extends all the way to the Pacific Coast), and the peaks of the Cascade Range to the east (Figure 1 and Figure 2). The study area makes up most of what is called the "Mid/Southern Willamette" valley. Elevations range from 0 m (0 ft) at the coast to 3,157 m (10,358 ft) at the peak of South Sister Mountain. The physiographic provinces in the study area include the Willamette River Valley, the Coast Range, and the Cascade Range. The Willamette Valley is characterized by predominately flat and gentle topography, while the Cascade Range and Coast Range are characterized by densely forested mountains. The convergence of the Cascade Range and the Coast Range mark the southern boundary of the study area.

The geology, topography, and climate of the study area are conducive to a number of natural hazards including floods, landslides, windstorms, volcanic eruptions, and earthquakes. The risks associated with earthquakes and landslides, in particular, are increasing as population continues to expand and to cause increased development.

The geology of the study area roughly matches the physiographic provinces (Figure 2 and Figure 3). The western portions within the Coast Range are composed of Tertiary volcanic and sedimentary rocks. The central portion contains the Willamette Valley, which is blanketed with unconsolidated Quaternary sediments. In the eastern portion of the study area the Cascade Mountains are formed mostly from Quaternary and Tertiary volcanic rocks and unconsolidated Quaternary alluvium. So, in even more general terms, there is loose material in the river valley and harder material in the Coast Range and Cascades.

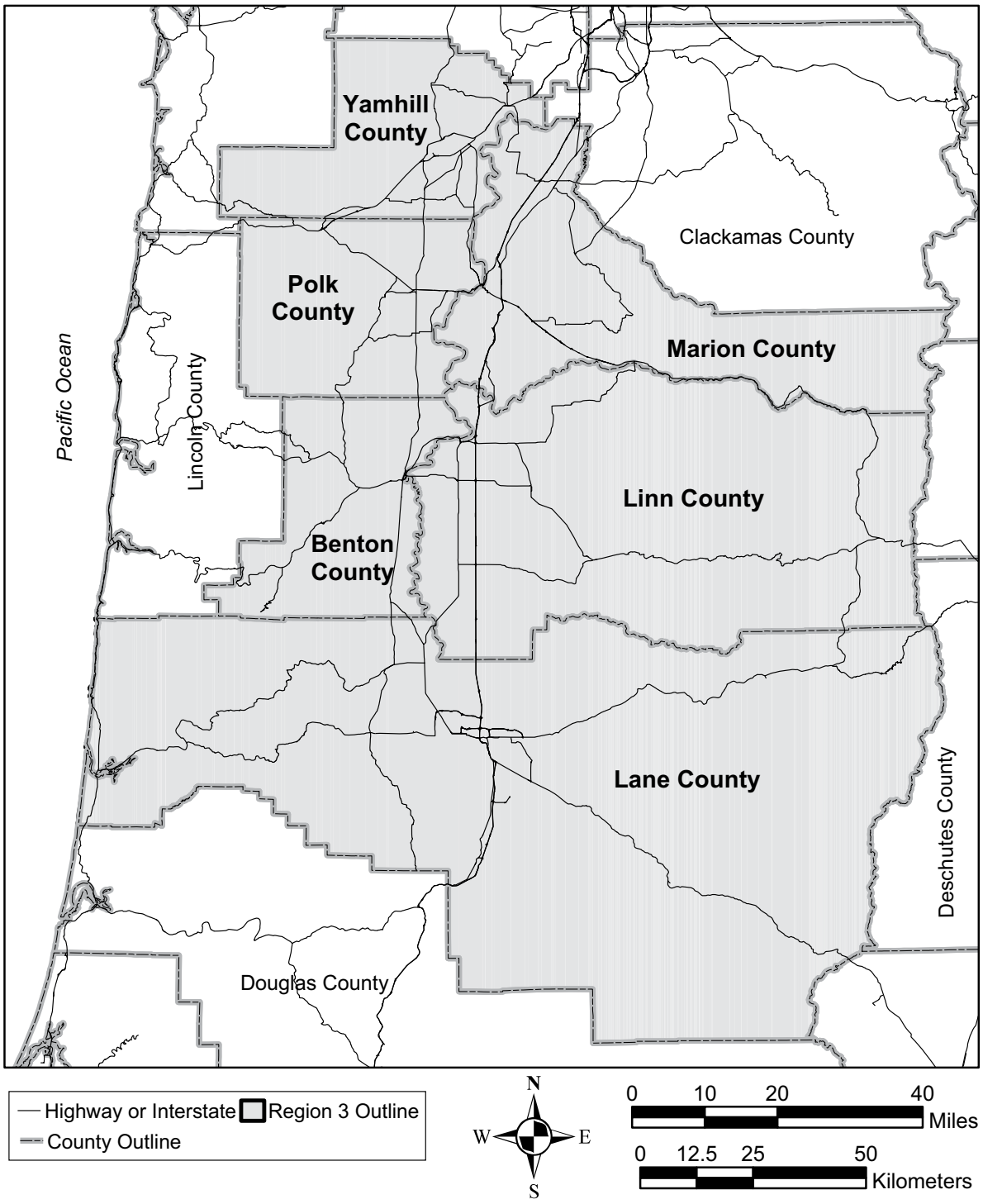

Figure 1. The study area (Oregon Partnership for Disaster Resilience Region 3) includes Yamhill, Polk, Marion, Benton, Linn, and Lane Counties, Oregon.

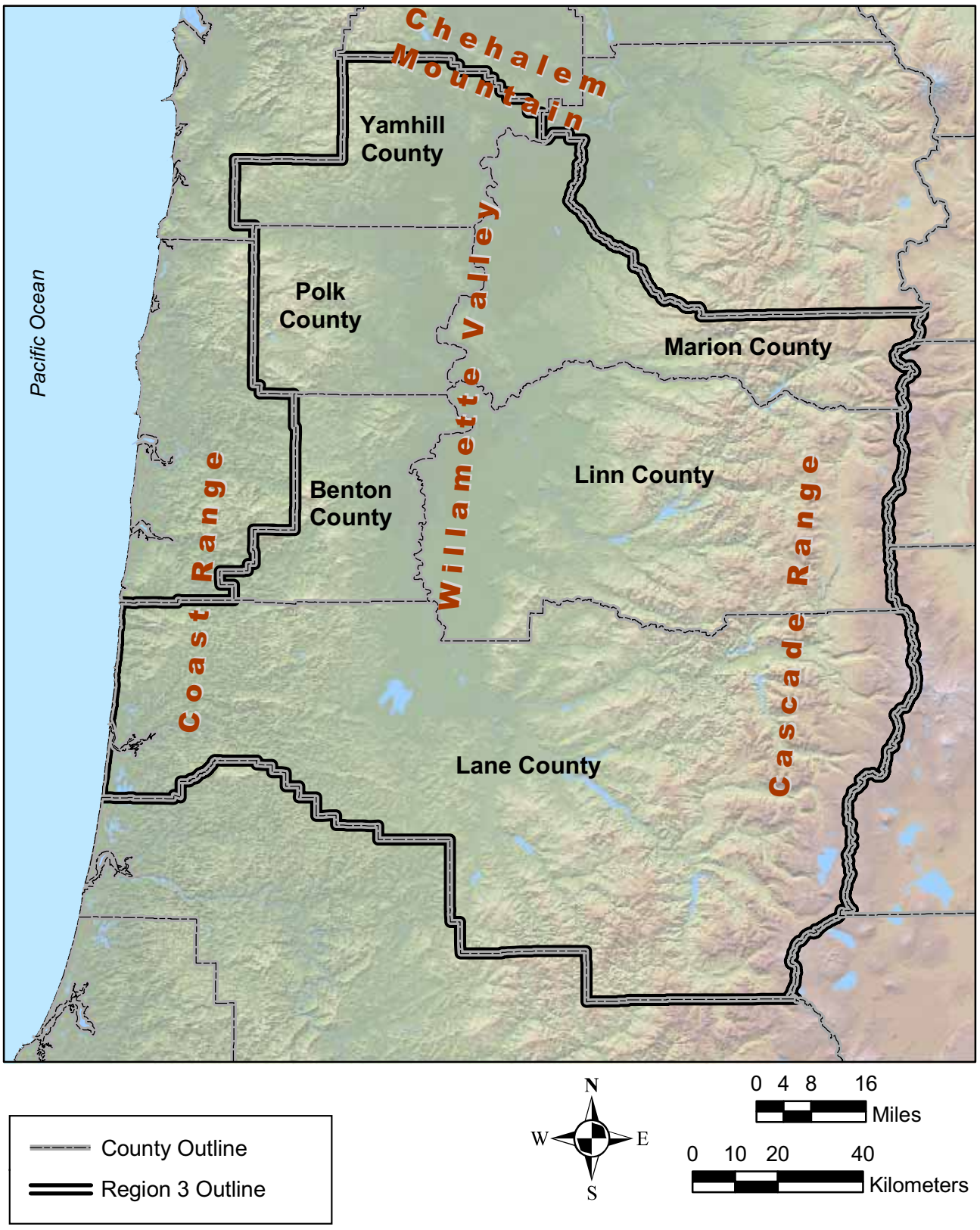

Figure 2. Shaded relief map of the study area with physiographic provinces including the Willamette Valley, the Coast Range, and the Cascade Range.

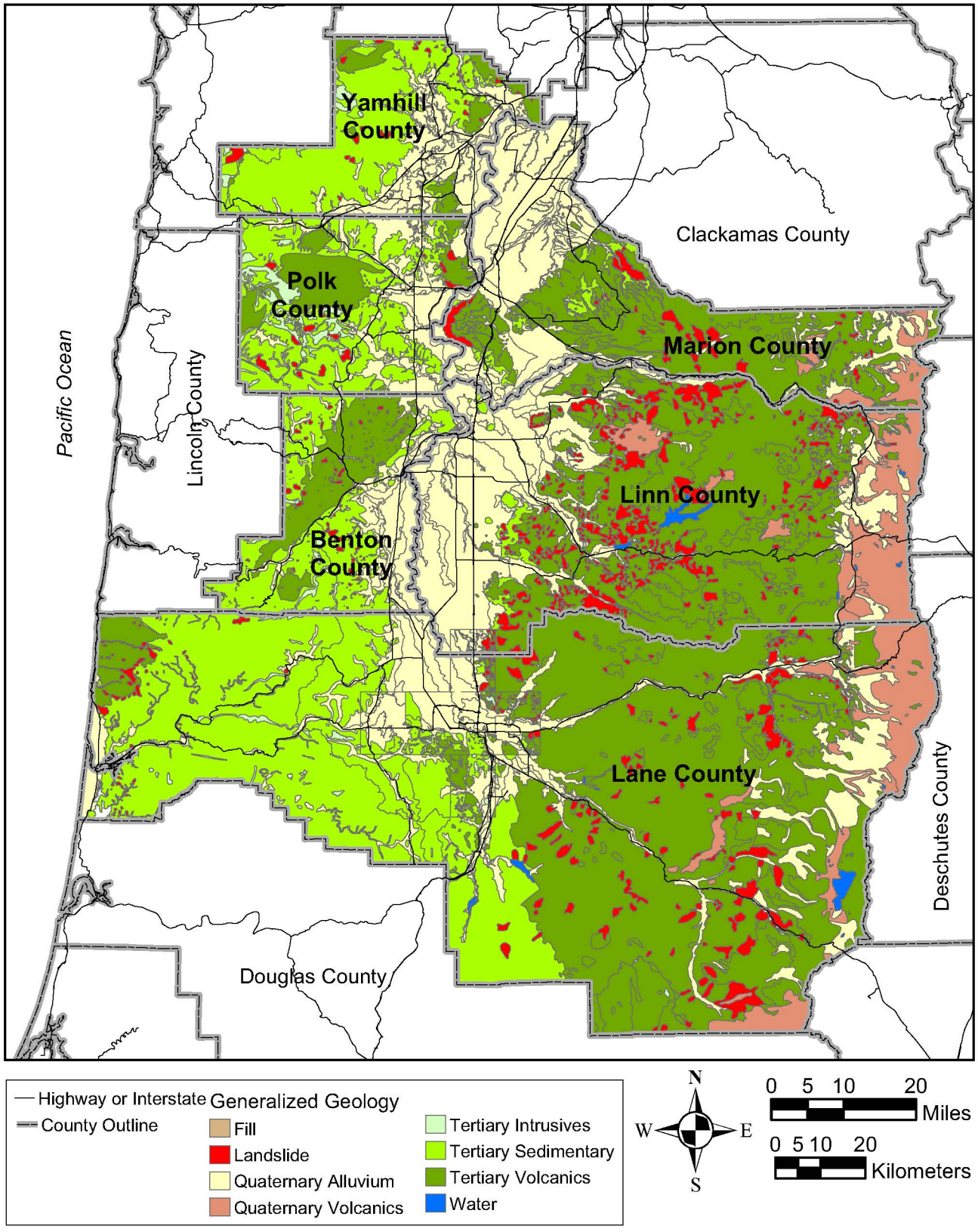

Figure 3. Generalized geologic map of the study area showing recent alluvium in the Willamette Valley (central portion of the map) and mostly Tertiary volcanics in the Cascade Range and Tertiary sedimentary rocks in the Coast Range.

5.0 GEOLOGIC HAZARDS

Several kinds of geologic hazards have the potential for major impact to communities within the study area. Earthquake-induced hazards include ground shaking, liquefaction, earthquake-induced landslides, and tsunamis. Deep-seated and rapidly moving landslides can occur on or adjacent to steep slopes. Earthquakes, landslides, and volcanic eruptions can trigger dam failures. Mount Jefferson and the Three Sisters region volcanic hazards pose specific threats in eastern Marion, Linn, and Lane Counties.

5.1 Potential Earthquake Sources and Earthquake-Induced Hazards

Earthquake effects are a significant threat in the study area and can come from subduction zone, intraplate, and crustal sources (Figure 4 and Figure 5).

5.1.1 Subduction Zone Earthquakes

Subduction zone earthquakes occur around the world where two tectonic plates meet and move toward each other, with one plate sliding (subducting) beneath the other. The subducted plate material melts and is reabsorbed in the mantle (Figure 4). The huge faults that separate the plates in these zones produce some of the most powerful earthquakes ever recorded, often having moment magnitudes of 8.0 to 9.0+. The 1960 Chilean (magnitude 9.5) and the 1964 Great Alaska (magnitude 9.2) earthquakes were subduction zone earthquakes. Both produced large tsunamis (Kanamori, 1977).

A magnitude 9.0 subduction zone earthquake located just off the west coast of Sumatra occurred December 26, 2004. This devastating earthquake occurred on the fault along which the India plate subducts beneath the overriding Burma plate and was the fourth largest earthquake in the world since 1900. It is estimated that

Figure 4. Schematic block diagram of the three earthquake sources: subduction, intraplate, and crustal.

250,000 people were killed and roughly 1,000,000 were displaced by the earthquake and subsequent tsunami in 10 countries in South Asia and East Africa (USGS Earthquake Program, 2004a). Three months later, on March 28, 2005, a second significant subduction zone earthquake with a magnitude of 8.7 shook the same region. Luckily, the epicenter of this earthquake was beneath shallow water and did not cause a significant tsunami (USGS Earthquake Program, 2005).

The Cascadia subduction zone, which lies off the Oregon and Washington coasts, is similar to the Sumatra area subduction zone. Though no earthquakes have been recorded on the Cascadia subduction zone during Oregon's short 200-year historical record, various studies have found widespread evidence that very large earthquakes have occurred, most recently about 300 years ago, in January 1700 (e.g., Atwater, 1987; Yamaguchi and others, 1997). The best available evidence and observations indicate that these earthquakes occur at intervals of about 200 to 1,000 years (Atwater and Hemphill-Haley, 1997).

5.1.2 Intraplate Earthquakes

Intraplate earthquakes occur in the Pacific Northwest within the Juan de Fuca plate as it subducts beneath the North American plate. Intraplate earthquakes have caused damage in the Puget Sound region in 1949, 1965, and 2001 (the 2001 event was the magnitude 6.8 Nisqually earthquake). These types of earthquakes typically occur at depths of 40–60 km (25–37 mi).

5.1.3 Crustal Earthquakes

Crustal earthquakes occur in the North American plate at relatively shallow depths of 10–20 km (6–12 mi) below the surface. The 1993 magnitude 5.6 earthquake at Scotts Mills, Oregon (Madin and others, 1993) and the 1993 magnitude 5.9 and 6.0 Klamath Falls, Oregon, main shocks (Wiley and others, 1993) are examples of crustal earthquakes.

The distance from a potentially active fault and a site is critical to the evaluation of the earthquake hazard. Figure 5 shows selected historical earthquake epicenters and known potentially active faults for the study area.

The U.S. Geological Survey (USGS) National Quaternary Fault and Fold Database (http://earthquake.usgs.gov/qfaults/) contains information on faults and folds in the United States that are believed to be sources of magnitude 6 and greater earthquakes during the Quaternary (the past 1,600,000 years). Maps of these geologic structures are linked to detailed descriptions and references as shown in Figure 6 (USGS Earthquake Program, 2004b).

Although the definition in Figure 5 of active faults is movement in the last 780,000 years, most scientists and engineers in the seismic field define active faults as having movement in the last 11,000 years or having multiple earthquakes during the Quaternary period.

The most severe damage inflicted by earthquakes is commonly associated with areas that experience one or more of the following phenomena:

- Amplification of ground shaking by soil columns
- Liquefaction of water-saturated sand, silt, or gravel, creating areas of "quicksand"
- Earthquake-induced landslides
- Tsunamis

Fortunately, each of these effects can be evaluated to a large extent before an earthquake occurs. The products of this study include maps of each of these earthquake hazards for each county and for the City of Albany.

5.1.4 Ground-Shaking Amplification

When an earthquake occurs, seismic waves radiate away from the epicenter and/or rupture zone. In general, the strength and duration of the shaking at a site is dependent on the size of the earthquake, distance away from the epicenter and/or rupture zone, and site-specific soil characteristics at the site. "In fact, ground shaking can be considered to be the most important of all seismic hazards because all the other hazards are caused by ground shaking" (Kramer, 1996, p. 2). This is true except for tsunami generation.

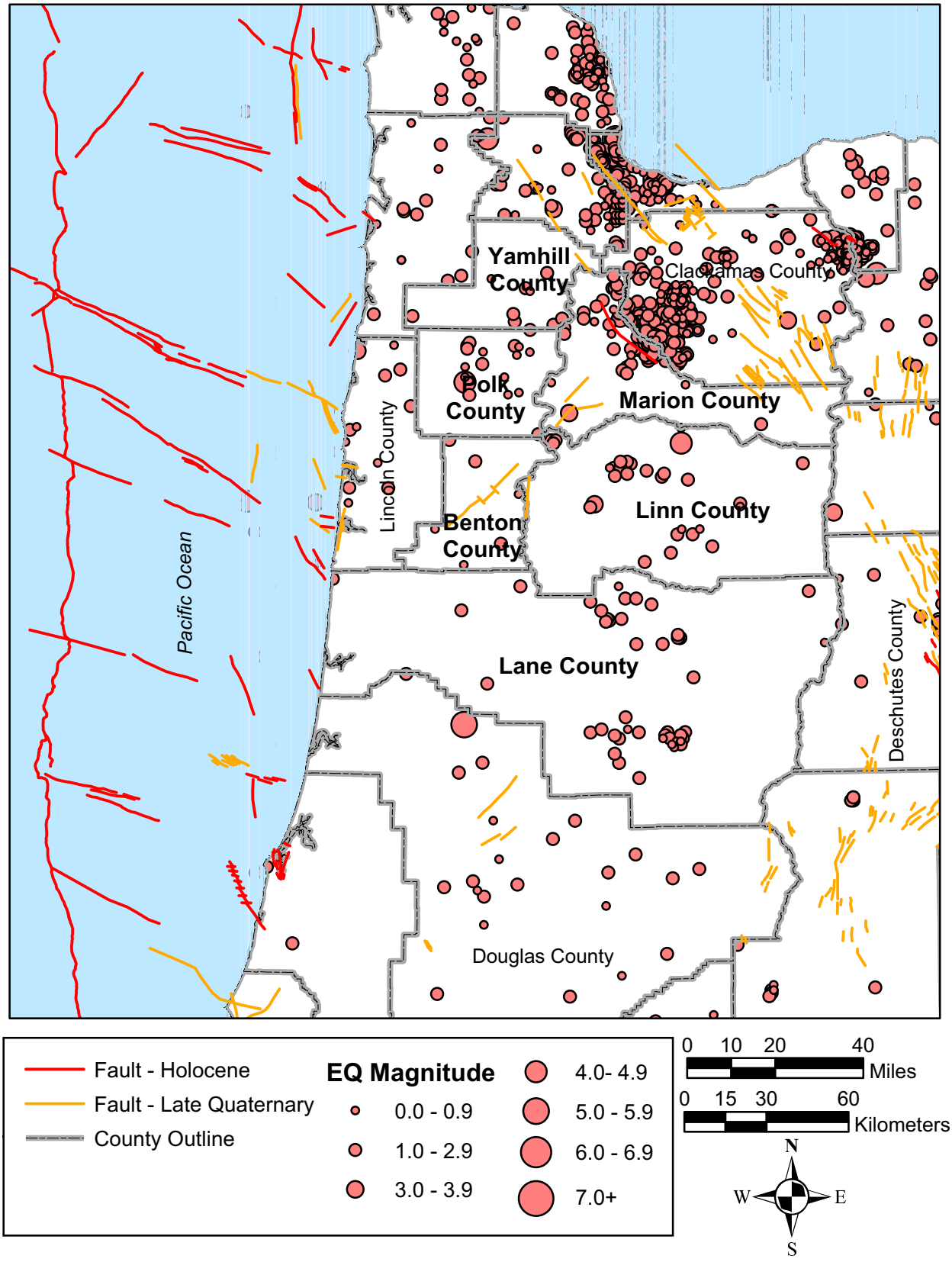

Figure 5. Map of selected historic earthquakes between 1841 and 2002 and Quaternary faults (from Niewendorp and Neuhaus [2003]). Active faults on this map are defined as those that have moved in the last 780,000 years (Geomatrix Consultants, Inc., 1995). Faults active in the last 20,000 years are colored red. Faults active between 20,000 and 780,000 years ago are colored gold.

USGS

Quaternary Fault and Fold Database for the United States

Salem 1° x 2° Sheet

Home > US Map > Oregon

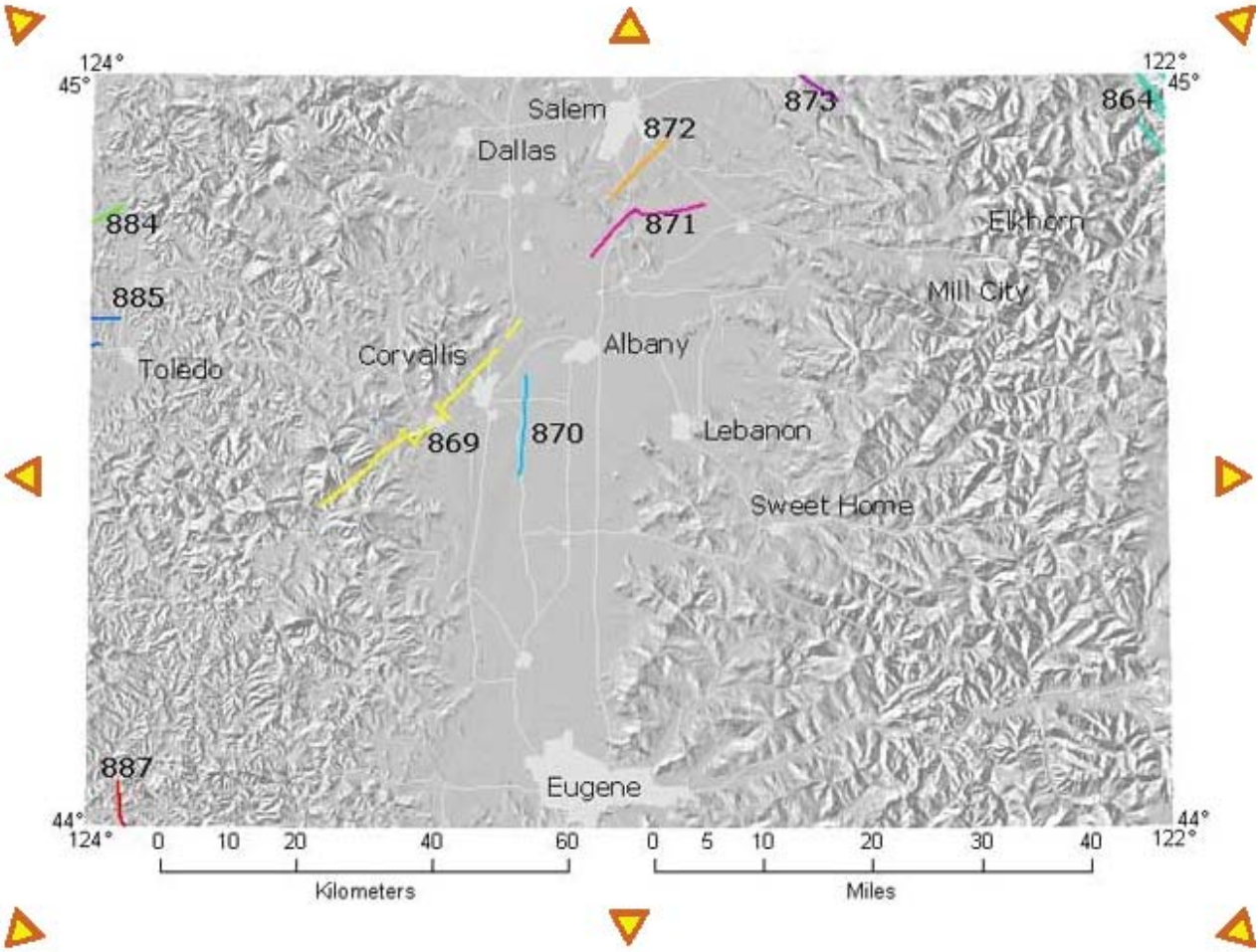

Number	Name
864	Clackamas River fault zone
869	Corvallis fault zone
870	Owl Creek fault
871	Mill Creek fault
872	Waldo Hills fault
873	Mount Angel fault
884	Cape Foulweather fault
885	Yaquina faults
887	Unnamed Siuslaw River anticline

Figure 6. Example of U.S. Geological Survey Quaternary fault and fold database output of the Salem 1° × 2° quadrangle (USGS Earthquake Program, 2004b).

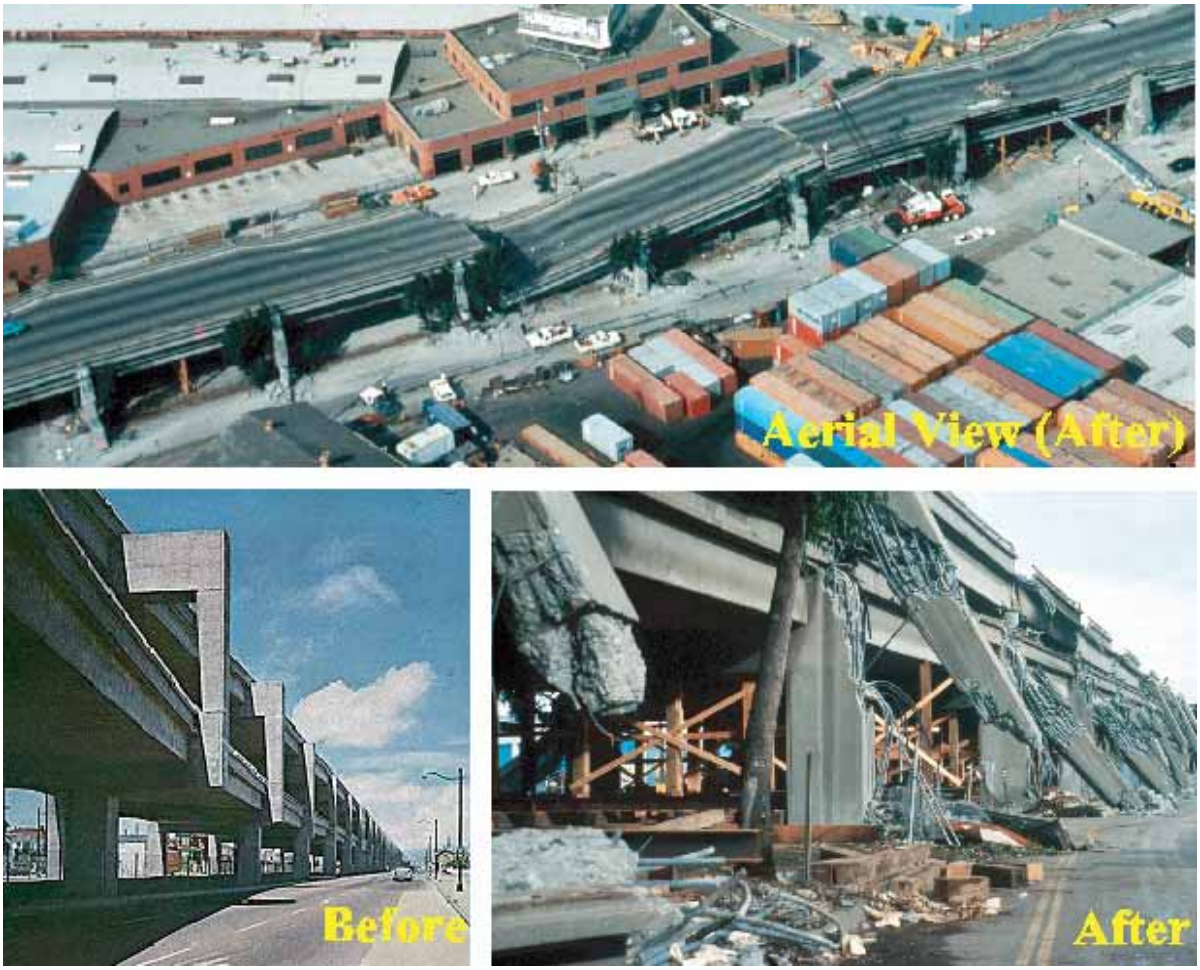

Figure 7. Example of damage to the Cypress viaduct of Interstate 880 caused by ground-shaking amplification during the October 17, 1989, Loma Prieta, California, earthquake (top: Nakata and Peterson, 1990) (bottom: Windmiller, 2000).

As seismic waves travel through bedrock, some energy propagates through surface soils to the ground surface. During propagation, soil deposits can either de-amplify (weaken) or amplify (strengthen) the shaking depending on the characteristics of the deposit. This phenomenon is generally referred to as ground-shaking amplification (GSA). Because soil deposits can change significantly over short distances, levels of ground-shaking amplification can also change markedly over a short distance, even if sites are at an equal distance from the earthquake source (Kramer, 1996).

Although earthquake site response is complicated and depends on factors such as frequency and duration of the shaking, subsurface stratigraphy and material properties, and surface topography, useful generalizations can be made about the performance of various soils. For example, thick deposits of soft soil tend to amplify the shaking of long-period ground motions, such as those associated with subduction zone earthquakes. In contrast, sites with thin soil profiles are not likely to amplify ground motions. The degree of amplification greatly affects the performance of structures during earthquakes; thus, substantially higher concentrations of damage are found in areas with high amplification factors (Holzer, 1994; Seed and others, 1988).

An example of ground-shaking amplification damage can be seen in the aftermath of the Loma Prieta, California, earthquake of October 17, 1989. Both the Cypress and the Embarcadero freeways were built on fill; in addition, the Cypress freeway was on an ancient streambed, not solid bedrock (Windmiller, 2000). During the earthquake, ancient streambed deposits

amplified the shaking, which partially caused the Cypress viaduct to collapse. Braces securing the upper level of the viaduct to the lower level broke and then split outward, sending the upper level down (Figure 7). The collapse started in the northern sections of the freeway, and each section collapsed until most of the viaduct was destroyed (Windmiller, 2000).

5.1.5 Liquefaction

During seismic shaking, deposits of loose, saturated sands can contract, resulting in an increase in pore water pressure. If the increase in pore water pressure is high enough (i.e., the effective stress equals zero), the deposit becomes "liquefied," losing its strength and thus its ability to hold support loads (Day, 2002; Kramer, 1996) (Figure 8).

If an earthquake induces liquefaction, several things can happen: 1) the liquefied layer and everything on top of it may move down slope, even on very gentle slopes, 2) the liquefied layer may oscillate with displacements large enough to rupture pipelines, move bridge abutments, or rupture building foundations, and 3) buoyant buried objects such as underground storage tanks can float toward the surface, and heavy objects such as buildings can sink. Typical displacements can range from centimeters to meters. Liquefaction can therefore significantly increase the damage resulting from an earthquake.

An example this kind of damage be seen in the aftermath of the Kawagishicho, Niigata, Japan, earthquake of 1964 (Figure 8). Settlement and tilt of apartment buildings due to liquefaction was very dramatic, although in many cases there was little structural damage.

Figure 8. (top) Example of liquefaction induced settlement of apartment buildings, Kawagishicho, Niigata earthquake, Japan, 1964 (Hausler and Sitar, 2001). (bottom) Example of a liquefaction sill at Hunting Island along the Columbia River. The sill most likely is a result of the last Cascadia Subduction Zone earthquake (in 1700 AD).

5.1.6 Earthquake-Induced Landslides

Strong ground shaking can also cause landslides and reactivate dormant landslides. Commonly, slopes that are marginally stable prior to an earthquake become unstable and fail. Some landslides result from liquefaction that causes lateral movement of soil, or lateral spread (Figure 9) (Kramer, 1996; Day, 2002). Section 5.2 contains describes non earthquake-induced landslides.

Figure 9. (top) Road prism rotational type landslide and (bottom) lateral spread landslide along the shoreline of Capitol Lake Olympia, Washington, caused by the 2001 magnitude 6.8 Nisqually earthquake (Nisqually Earthquake Information Clearinghouse, 2001).

5.1.7 Tsunamis

Tsunamis are caused by large-scale disturbance of the sea floor. During a subduction zone earthquake the sea floor is uplifted. This in turn uplifts the overlying column of water, forming the initial tsunami wave. Tsunamis can arrive at nearby coastlines in minutes, causing extensive damage and loss of life, as recently occurred in Indonesia in December 2004 (Figure 10). Subduction zone earthquakes also typically cause landslides that can greatly amplify tsunami runup, should the landslides occur under the sea or slide from land into water (Priest, 1995).

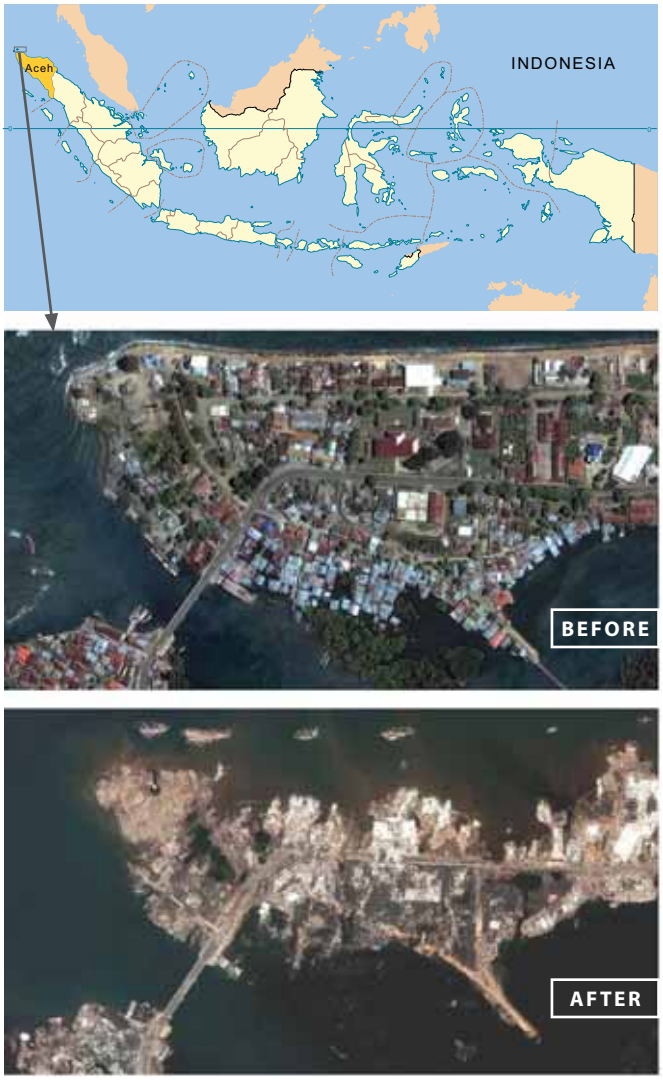

Figure 10. Devastation caused by tsunami waves is shown in "before" and "after" aerial photographs of an island off the northern tip of the Aceh province of Indonesia (photographs copyright DigitalGlobe, 2004).

5.2 Landslide Types and Characteristics

Landslides pose a significant hazard in the study area and can take many different shapes and forms. Landslides in the United States cause an average of 25 to 50 deaths and $1 to $2 billion in economic losses annually (Schuster and Fleming, 1986). In Oregon, a minimum estimated $10 million in damage occurs annually (Wang and others, 2002). During 1996 and 1997, heavier than normal rains caused over 700 landslides in the Portland metropolitan area, which cost more than $40 million to mitigate (Burns, 1999).

5.2.1 Landslide Types and Trigger Mechanisms

The general term landslide refers to a range of geologic failures including rock falls, debris flows, earth slides, and other mass movements (Figure 11). Most slope failures in the study area are complex combinations of these distinct types, but generalized groupings provide a useful means for framing discussion of slide characteristics, identification methods, and potential mitigation alternatives. Landslides can be initiated in marginally stable slopes by a number of natural and human disturbances. Processes and conditions that can trigger slope failure include earthquake shaking, volcanic eruptions, deforestation and deforestation-related activities such as road building, and rapid snow melt (Turner and Schuster, 1996). Two of the most common triggering events in the Pacific Northwest are intense rainfall and man-made changes to land.

In the Pacific Northwest region, large and devastating landslides in and around Kelso, Washington, have captured national attention. A massive landslide began to move in 1998 and destroyed almost half of the 137 houses in the Aldercrest subdivision (Figure 12).

Of the 700 landslides recorded during 1996 in Portland, Oregon, metropolitan region by Burns and others (1998), 76% were caused or exacerbated by human activity. In a similar study in and around Seattle, Washington, man-made alterations were associated with over 75% of the recorded landslides (W. D. Nashem and W. T. Laprade, update on the Seattle landslide inventor, electronic mail distribution, 1999).

The mechanics of slope stability can be divided into two forces: driving forces and resisting forces. These forces are a function of the material properties and the geometry of the slope. These two forces oppose each other, and slope stability can be thought of as their ratio (Burns and others, 1998).

$$\text{factor of safety} = \frac{\text{resisting forces}}{\text{driving forces}}$$

A ratio greater than 1 indicates a stable slope because the resisting forces are greater than the driving forces. A ratio less than 1 indicates an unstable slope because the driving forces are greater than the resisting forces. A critically stable slope would have a ratio equal to roughly 1. However, because not all conditions present within a slope can be accounted for, Senneset (1996) recommends that slopes with a factor of safety of less than 1.3–1.5 be considered potentially unstable (Burns, 1999).

Prior to developing remedial measures for slope instability on a site-specific basis, it is helpful to have a solid grasp of the regional tendency for landslide activity based on a synthesis of geologic, topographic, climatological, and historical data. The maps developed in this study allow for systematic, objective evaluations of slope hazards at a regional scale. These evaluations can lead to identification of specific sites that warrant attention, a fundamental goal of this project.

One potentially devastating type of landslide is a channelized debris flow or "rapidly moving landslide." This type of flow initiates upslope, moves into or transports down a steep channel (or drainage), then deposits its material, usually at the mouth of the channel. Debris flows can be initiated by other types of landslides that occur on slopes near a channel. They can also initiate within the channel in areas of accelerated erosion during heavy rainfall or snowmelt.

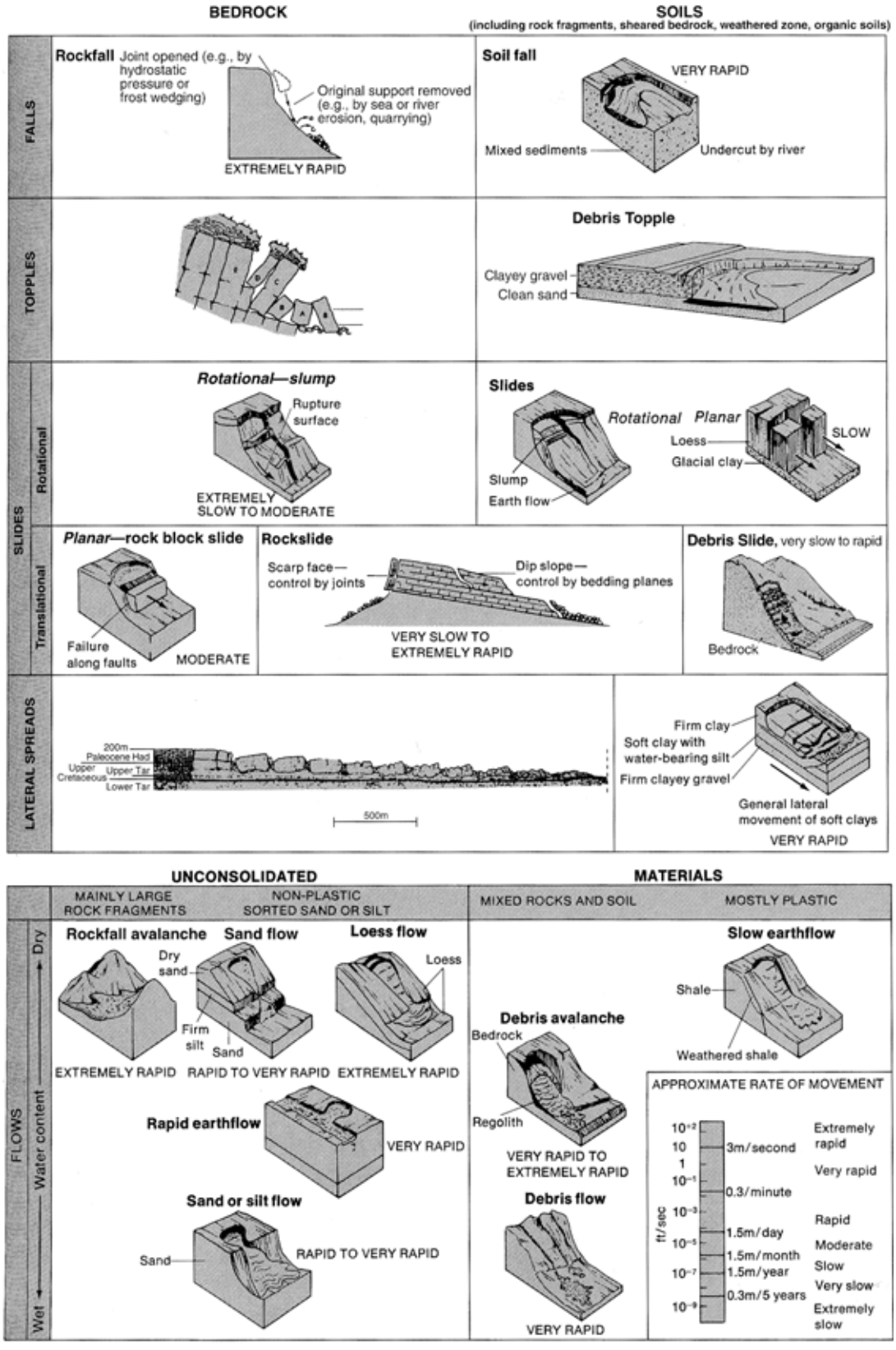

Figure 11. Landslides can be categorized by material type, type of movement, relative water content, and rate of movement (from Ritter and others, 1995).

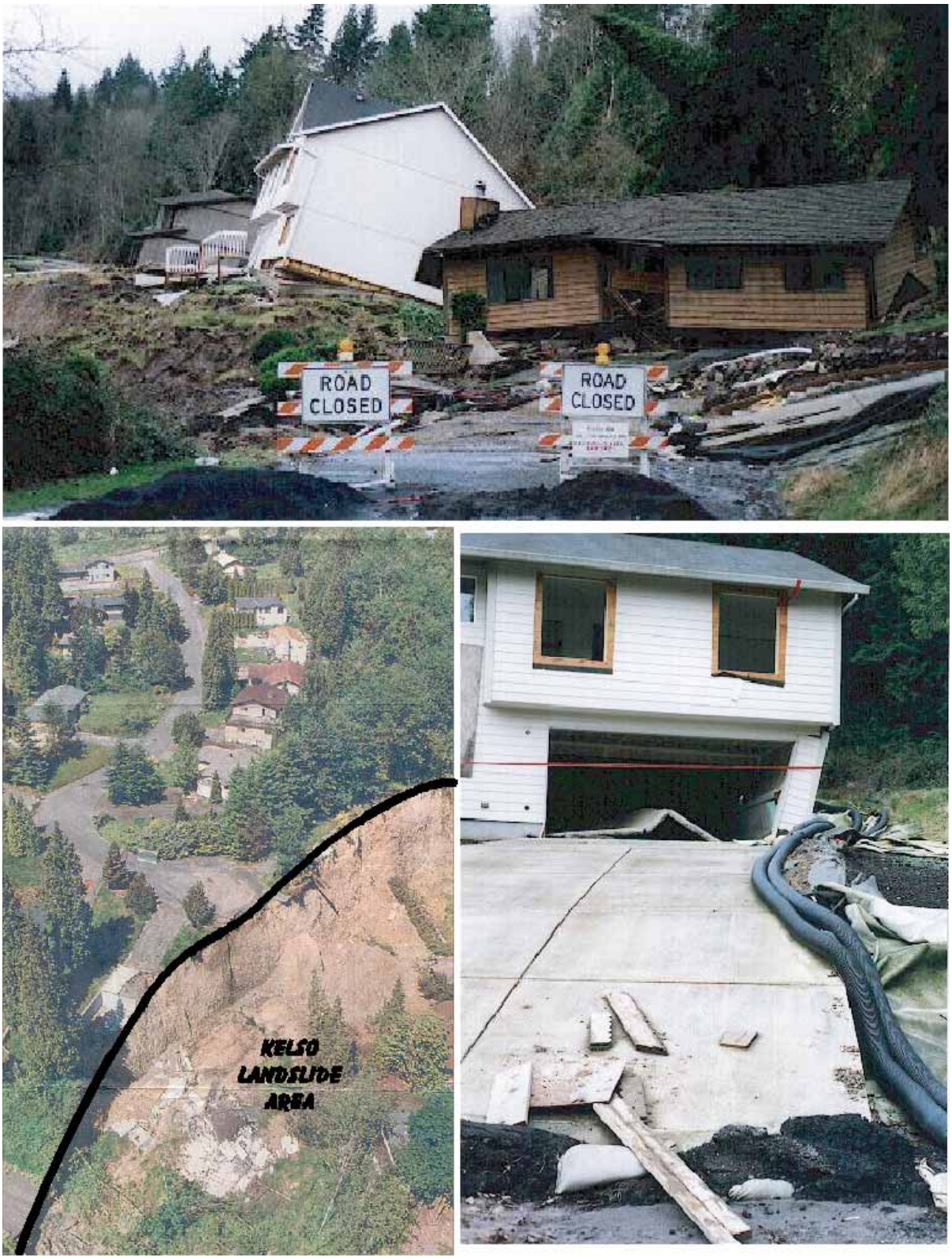

Figure 12. Destruction from the Kelso, Washington, landslide that initiated in 1998. (top) Houses have been tilted and pulled apart. (left) Aerial view of the head scarp area. (right) Concrete driveway has "bulldozed" the asphalt and the garage slab has been uplifted. Photographs were taken between January 1999 and June 2000 (NW Geoscience.com, 2002).

5.3 Other Geologic Hazards

5.3.1 Volcanic Hazards

Paralleling the coast of northern California, Oregon, Washington, and southern British Columbia is a chain of volcanoes, which are part of the Cascade Range. These volcanoes exist because the Juan De Fuca oceanic plate subducts below the North American plate (continental crust), where the rock becomes molten at depth and rises to the surface to erupt as volcanoes (Figure 4 and Figure 13). Mount Saint Helens, a volcano in this chain, erupted violently in 1980. The volcano erupted steam and ash again during fall 2004 and spring 2005, with activity continuing intermittently.

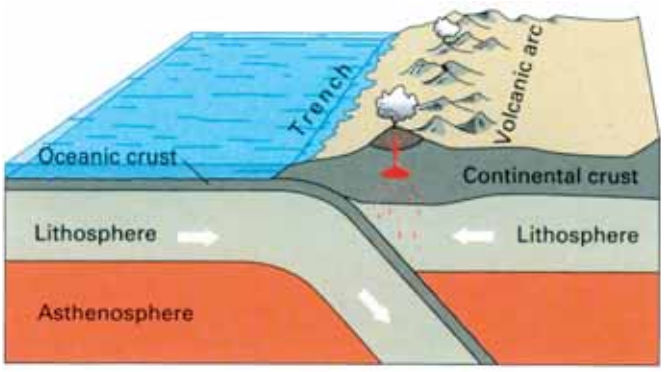

Figure 13. Converging plate margin schematic displaying the relationship between the subducting plate and the resulting volcanic arc.

Volcanic activity can produce many types of hazardous events including landslides, fallout of tephra (volcanic ash), lahars, pyroclastic flows, and lava flows (Figure 14) (Scott and others, 1999). Pyroclastic flows are fluid mixtures of hot rock fragments, ash, and gases that can move down the flanks of volcanoes at speeds of 50 to more than 150 kilometers per hour (30 to 90 miles per hour) (Scott and others, 1999). Lahars or volcanic debris flows are water-saturated mixtures of soil and rock fragments and can travel very long distances (over 100 km) and travel as fast as 80 kilometers per hour (50 miles per hour) in steep channels close to a volcano (Scott and others, 1999). These hazards can affect very small local zones (only meters across) to areas hundreds of kilometers downwind (Walder and others, 1999).

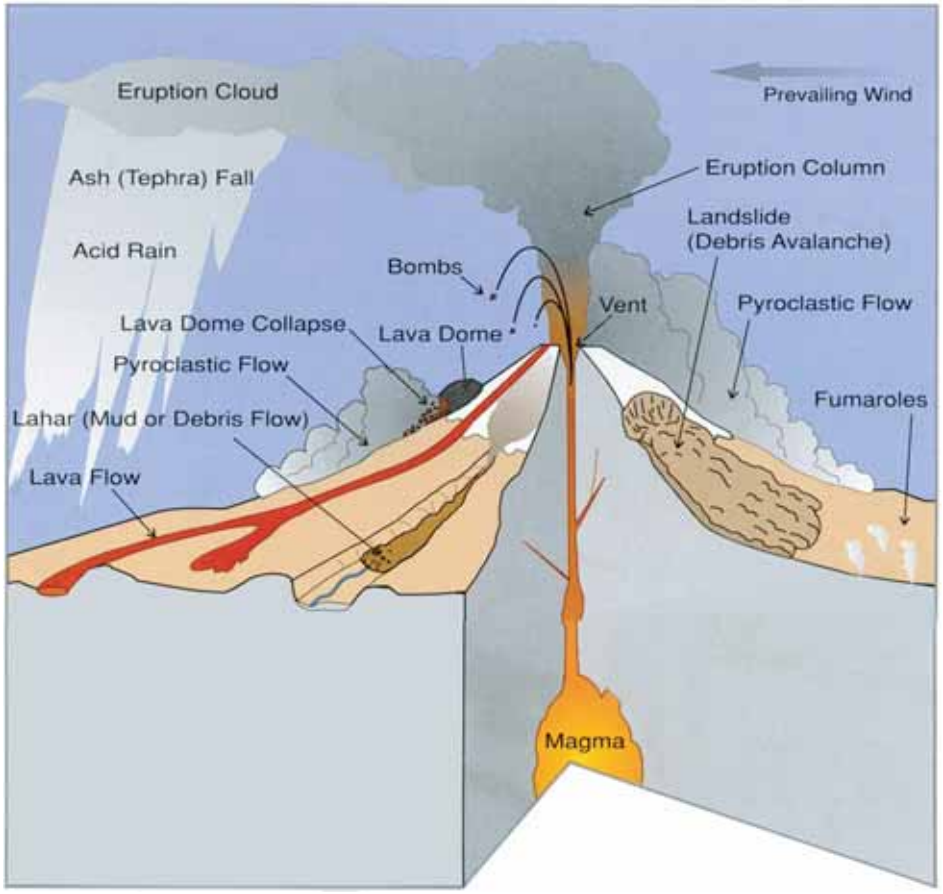

Figure 14. Volcanic hazard from a composite type volcano (Scott and others, 1999).

5.3.2 Dam Failure

The U.S. Army Corps of Engineers maintains a database (National Inventory of Dams; NID) of all dams in the United States that have a high or significant hazard potential or low hazard with certain other criteria such as dam height or storage volume (Goettel and others, 2004). The NID hazard classification is related only to impact if a dam fails, not dam safety level or likelihood of failure. In other words, a "high hazard dam" simply means that people downstream from the dam in the inundation area are at risk. Since 1874, there have been six large-impact dam failures in the United States, and each caused greater than 100 deaths. The worst dam failure, in terms of casualties, was the 1889 Johnstown, Pennsylvania, dam failure, which killed over 2,200 people.

Two geologic hazards are mainly associated with potential dam failure: landslides and earthquakes. If a landslide moves debris into a reservoir, a local tsunami wave could be generated and could cause the dam to fail. After dam failure and the related fast drawdown of water in the reservoir, it is very common to have many landslides into the now empty reservoir. Landslides can also directly impact the dam itself. The Seminary Hill Reservoir dam, located within the City of Centralia, Washington, failed October 5, 1991; the failure was caused by a massive landslide in the siltstone rock formation that underlies the reservoir (Figure 15) (Washington State Department of Ecology, Water Resources, 1991).

A major earthquake, either a Cascadia Subduction Zone earthquake or a smaller, crustal or intraplate earthquake, could also cause sufficient damage to a dam and pose a risk of failure. Most dams in Oregon were designed and built in the 1940s to 1960s, when seismic design considerations were significantly lower than they are now (Goettel and others, 2004).

Figure 15. Seminary Hill Reservoir dam failure caused by a landslide. Portions of the City of Centralia, Washington, were inundated. (Washington State Department of Ecology, Water Resources, 1991).

6.0 GEOLOGIC HAZARD MAPS

Although the specific location and the exact timing of natural hazard events are difficult to forecast, we do have tools for planning and forecasting. Historical observations of natural hazards coupled with significant advances in computer modeling and GIS capabilities allow us to map potential hazards over large areas.

The following sections briefly describe the GIS map layers that communities can use to identify regional natural hazard areas. Maps in the list below denoted with asterisks were produced in this study; county maps are provided in appendices A–G. The other listed maps come from previous studies.

- Ground-shaking amplification *
- Liquefaction *
- Tsunami inundation zone map
- Earthquake-induced landslides *
- Identified landslide areas *
- Inventory of slope failures in Oregon from three storm events (1996-1997)
- Map of potential "rapidly moving landslide" or debris flow hazards
- Volcanic hazard maps
- Dam failure inundation and hazard maps

For Benton County we used existing countywide hazard layers provided by DOGAMI Open-File Report O-01-05 (Wang and others, 2001) except the identified landslide map, which we improved from the 2001 version and which is included.

6.1 Ground-Shaking Amplification Map

A commonly used method of categorizing regional ground-shaking amplification hazards was developed by the National Earthquake Hazard Reduction Program (NEHRP) (FEMA, 2003b). The NEHRP 2003 method classifies local geology into one of six categories generally labeled hard rock (type A), rock (type B), very dense soil and soft rock (type C), stiff soils (type D), soft soils (type E), and soils requiring site-specific evaluations (type F).

Table 1 summarizes some of the defining characteristics of these categories. Because site-specific information is needed to classify soils as type F, this class was lumped with the type E soils in this study; furthermore, type F soils may also be located within other classes.

Table 1. National Earthquake Hazards Reduction Program ground-shaking amplification site classes (FEMA, 2003b) and corresponding DOGAMI ground-shaking amplification hazard classes used in this study.

Site Class	Site Class Description	Shear Wave Velocity, $\bar{v}_s$ (m/s) Min.	Max.	DOGAMI Hazard Class
A	**Hard Rock**	1500	—	very low
B	**Rock**	760	1500	low
C	**Very Dense Soil and Soft Rock.** $s_u \geq$ 2,000 psf (100 kPa) or $N > 50$	360	760	moderate
D	**Stiff Soils** (stiff soil with undrained shear strength). 1,000 psf ≤ s_u ≤ 2,000 psf (50 kPa ≤ s_u ≤ 100 kPa) or 15 ≤ N ≤ 50	180	360	high
E	**Soft Soils**. Profile with more than 3 m of soft clay defined as soil with $PI > 20$, moisture content $w > 40\%$, and undrained shear strength $s_u <$ 2,000 psf (50 kPa) ($N <$ 15 blows/ft)	—	180	very high*
F	**Soils Requiring Site-Specific Evaluations** 1. Soils vulnerable to potential failure or collapse under seismic loading such as liquefiable soils, quick and highly sensitive clays, collapsible weakly cemented soils. 2. Peat and/or highly organic clays ($H > 3$ m of peat and/or highly organic clay) 3. Very high plasticity clays ($H > 8$ m with PI > 75) 4. Very thick, soft/medium stiff clays ($H > 36$ m) with $s_u <$ 1,000 psf (50 kPa)	—	—	

Min. is minimum, Max. is maximum, s_u is undrained shear strength; N is ; PI is plasticity index; H is soil thickness.
*Note that because site-specific information is needed to classify soils as type F, this class was lumped with the type E soils in this study; furthermore, type F soils may also be located within other hazard classes.

We developed the ground-shaking amplification maps based generally on the NEHRP 1997 method of categorizing site geology. As explained in more detail in Appendix H, we started by geographically combining available GIS data from previous hazard studies with surface geology layers. We then assigned NEHRP 1997 susceptibility classes based on the dominant lithologies for each geologic unit in the study area.

The resulting maps are not intended to be used in place of site-specific studies. The simple five-class scale of Very Low, Low, Moderate, High, and Very High on the maps corresponds to the NEHRP site classes as shown in Table 1. These classes are the relative amount of expected ground-shaking amplification at the site. No type A areas were mapped within the study area (type A profiles are not common on the west coast of the United States). In addition to the regional hazard maps developed for this study, some existing local hazard maps were used to override the generalized regional maps. Most of these existing maps were produced for the major cities in the study area and include DOGAMI publications IMS-7, -8, -9, -10, -14, -17, -18, and Open-File Report O-01-05. For Benton County (Open-File Report O-01-05) the existing amplification GIS layers developed by DOGAMI (Wang and others, 2001) were subjected to the same GIS topology cleanup process as the files developed in this study.

A version of the resulting GIS map layer is shown as Figure 16. In general, areas characterized by loose, Quaternary sedimentary deposits are mapped as Moderate and High hazard for ground-shaking amplification (mostly D, E, and F type soil profiles). Most areas adjacent to major rivers in the more populated central portion of the study area are mapped as High and Very High hazard. Upland areas in the eastern part of the study area are mapped as Low ground motion amplification hazard, reflecting bedrock exposures and thin mantles of soil overlying rock. The western portion of the study area is varied, with competent bedrock areas mapped as Low hazard, dense soil areas mapped as Moderate hazard, and younger landslide and alluvial deposit areas mapped as High hazard for ground-shaking amplification.

6.2 Liquefaction Hazard Map

Liquefaction hazards can be evaluated several ways, but for regional mapping it is common to assess hazards using a classification system developed by Youd and Perkins (1978). Table 2 summarizes the liquefaction susceptibility rating system developed by Youd and Perkins (1978). The method takes into account the geologic environment of soil deposition and the general age of deposits. Again, as with ground-shaking hazards, several existing hazard maps produced at local levels were used to override the regional maps developed in this study. Because most of these geologic maps did not make a distinction between cohesionless (i.e., sand) and cohesive (i.e., silt and clay) materials (in fact, most map unit descriptions included both), the deposit types listed in Table 2 were used in a very general way to classify all of these deposits. The steps used to develop the liquefaction hazard map and original data sources are provided in Appendix H.

We assigned liquefaction susceptibility classes based on the dominant lithologies for each geologic unit in the study area and simplified the GIS output into six relative hazard classes: Rare (includes bedrock units older than Pleistocene; not included in Table 1), Very Low, Low, Moderate, High, and Very High.

A version of the GIS map layer for liquefaction hazards is shown as Figure 17. Areas with Moderate to High liquefaction susceptibilities are concentrated along the rivers and flood plains in the Willamette Valley, Cascade Range tributaries, and major stream valleys within the Cascade Range. We assigned older river terrace deposits in the Willamette Valley a lower liquefaction hazard, but we still consider these deposits to be susceptible to liquefaction during larger earthquakes. It is important to note that the quality and scale of the available geologic base maps precluded identification of all liquefaction hazard areas.

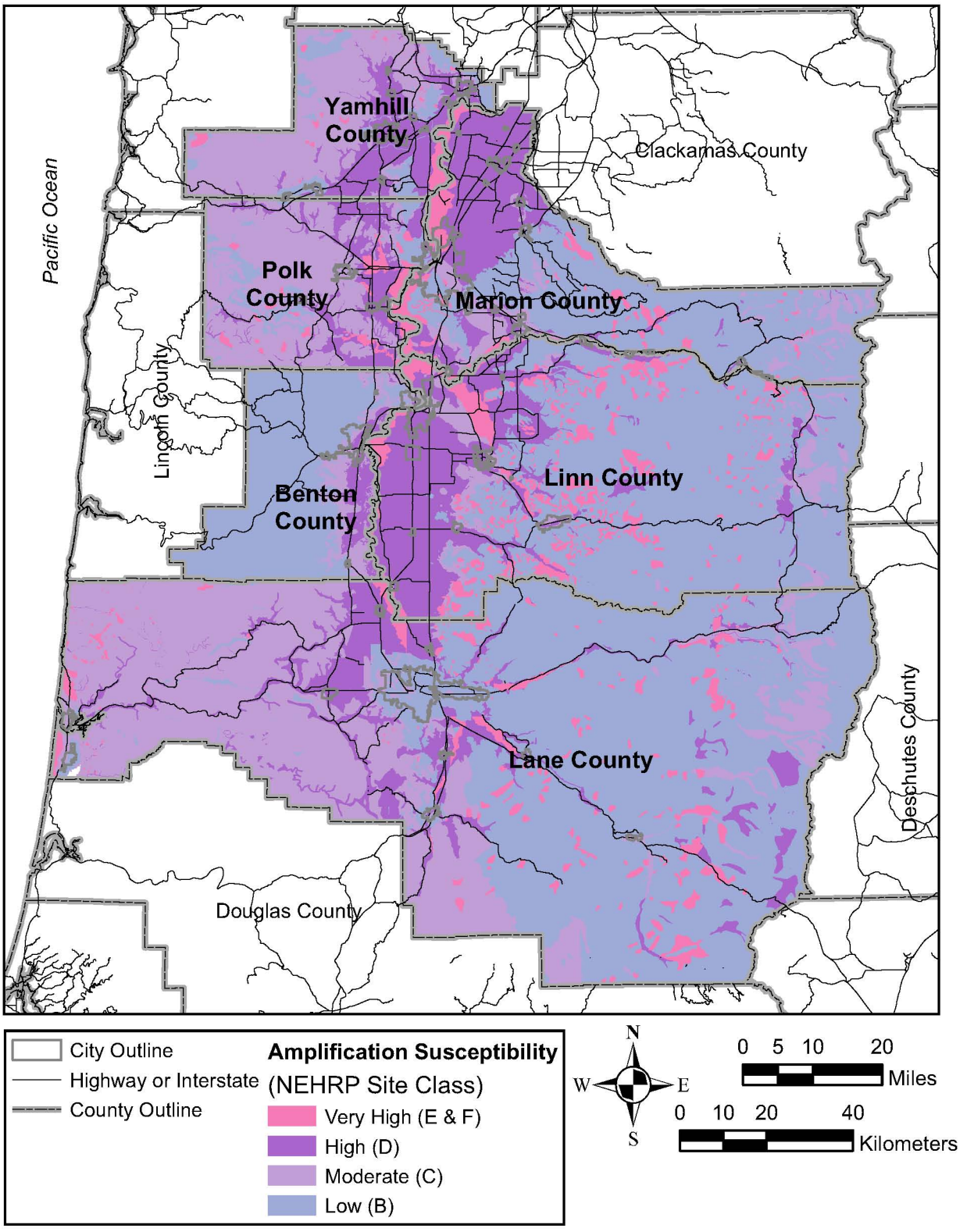

Figure 16. Ground-shaking amplification hazard map for the study area. The simple five-class scale of hazard classes generally corresponds to NEHRP classes. No type A areas were mapped within the study area (type A profiles are not common on the west coast of the United States). Benton County data were modified from Wang and others (2001).

Table 2. Liquefaction susceptibility rating system (from Youd and Perkins [1978]).

Type of Deposit	General Distribution of Cohesionless Sediments in Deposits	Likelihood That Cohesionless Sediments When Saturated Would Be Susceptible to Liquefaction (by Age of Deposit)			
		Modern < 500 yr	Holocene < 11 ka	Pleistocene 11 ka - 2 Ma	Pre-Pleistocene > 2 Ma
(a) Continental Deposits					
River channel	locally variable	very high	high	low	very low
Flood plain	locally variable	high	moderate	low	very low
Alluvian fan and plain	widespread	moderate	low	low	very low
Marine terraces and plains	widespread	—	low	very low	very low
Delta and fan-delta	widespread	high	moderate	low	very low
Lacustrine and playa	variable	high	moderate	low	very low
Colluvium	variable	high	moderate	low	very low
Talus	widespread	low	low	very low	very low
Dunes	widespread	high	moderate	low	very low
Loess	variable	high	high	high	unknown
Glacial till	variable	low	low	very low	very low
Tuff	rare	low	low	very low	very low
Tephra	widespread	high	high	?	?
Residual soils	rare	low	low	very low	very low
Sebka	locally variable	high	moderate	low	very low
(b) Coastal Zone					
Delta	widespread	very high	high	low	very low
Esturine	locally variable	high	moderate	low	very low
Beach					
High wave energy	widespread	moderate	low	very low	very low
Low wave energy	widespread	high	moderate	low	very low
Lagoonal	locally variable	high	moderate	low	very low
Fore shore	locally variable	high	moderate	low	very low
(c) Artificial					
Uncompacted fill	variable	very high	—	—	—
Compacted fill	variable	low	—	—	—

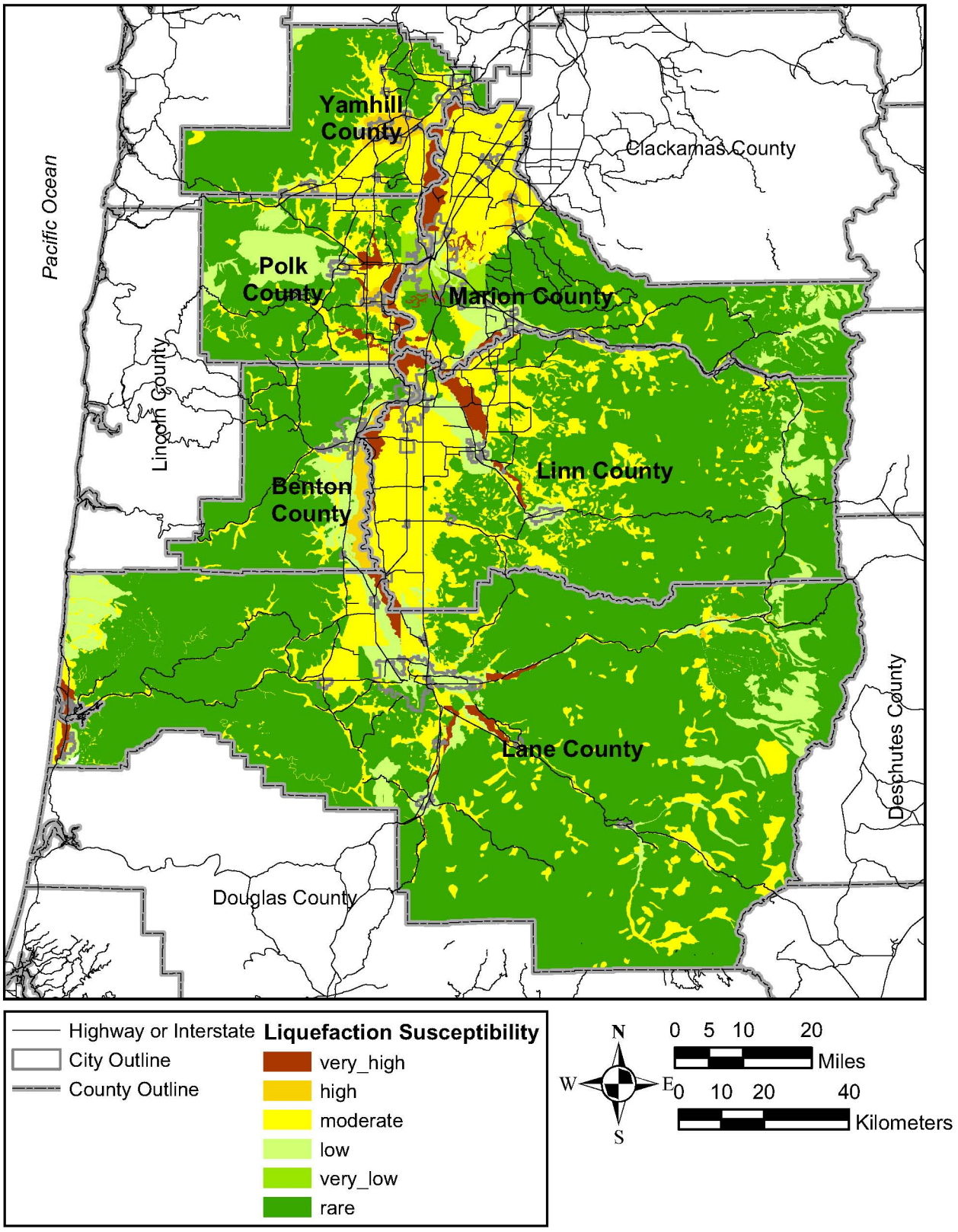

Figure 17. Liquefaction hazard map for the study area displays the six liquefaction potential classes used in this study. Benton County data were modified from Wang and others (2001).

6.3 Tsunami Hazard

Tsunamis are caused by large-scale disturbance of the sea floor. The most common cause is the concurrent uplift and subsidence of sea floor caused by great subduction zone earthquakes. The shape of the deformed sea floor is transmitted to the overlying sea surface, forming the initial tsunami wave that can arrive at nearby coastlines in minutes, causing extensive damage and loss of life. Subduction zone earthquakes also typically cause submarine landslides that can greatly amplify tsunami runup. This latter hazard is not directly addressed here but could be an important consideration when adding factors of safety for evacuation planning (Priest, 1995). Priest (1995) produced tsunami inundation maps by modeling the deformation from an earthquake, numerically simulating the resulting waves, and mapping the maximum inland flooding limit (inundation zone) (Figure 18) on 1:24,000 scale topographic maps. The inundation limit takes into account the effects of expected coseismic subsidence estimated from the study of wetland soils buried during prehistoric earthquakes.

6.4 Landslide Hazard Maps

In this study, we used a combination of approaches to develop two new landslide hazard identification products. The first new product is a regional earthquake-induced landslide hazard map (see subsection 6.4.1) that distinguishes different areas on the basis of the simple combination of slope gradient derived from a 10-m digital elevation model (DEM)[1] and generalized material type (USGS, 2004). The second new product is a GIS compilation of identified landslide areas (see subsection 6.4.2) derived from published geologic reports and geohazards studies.

Two previously prepared landslide hazard maps are included in this report. The first is a GIS database of known landslide locations (point and polyline features) from previous DOGAMI compilation efforts following the 1996-1997 Oregon major storm events (Hofmeister, 2000) (see subsection 6.4.3). The second existing product is a regional debris flow or "rapidly moving landslide" hazard map (see subsection 6.4.4) (Hofmeister and others, 2002).

6.4.1 Earthquake-Induced Landslide Map

We prepared the regional earthquake-induced landslide hazard map using an approach similar to the Wilson and Keefer (1985) methodology employed within HAZUS-MH. The method combines two important factors relating to landslide susceptibility: slope gradient and geologic material strength (relative slope instability susceptibility). In regional applications such as this study, slope gradient is derived from digital elevation models (in this case, a 10-m DEM). We estimated material strength by grouping geologic units into three simple geologic groups — Low, Moderate, and High — based on the unit characteristics identified in the geologic reports and our comparisons with other landslide hazard information. We assigned the vast majority of units to the Medium material class (highly weathered rock and unconsolidated sediments); only units with substantially divergent characteristics were assigned to the Low (consolidated bedrock) and High (existing landslides) classes. The steps used to develop the earthquake-induced landslide hazard map and original data sources are provided in Appendix H.

We assigned hazard classes of Low, Moderate, High, and Very High from the combination of slope map and geologic group categories as shown in Table 3. We developed these categories specifically for this project, although the table reflects a structure similar to that of Wilson and Keefer (1985) within HAZUS-MH.

The resulting landslide hazard map with relative designations Low, Moderate, High, and Very High is shown in Figure 19. The relative hazard map depicts locations of higher and lower relative hazard based on general material type and slope at 10-m grid spacing. Steep slopes tend to dominate the higher hazard zones throughout the counties. Many mountainous areas are identified as having an elevated landslide hazard, but steeper portions of the lowland Willamette Valley also have elevated landslide hazards. For example, areas of historic landslide activity such as along the banks

1 A DEM is a digital representation of topography, usually consisting of a grid (a regularly spaced series of points) with elevation values assigned to geographic coordinates (such as latitude, longitude). The grid spacing (10 m in this case) refers to the map view distance between the grid points.

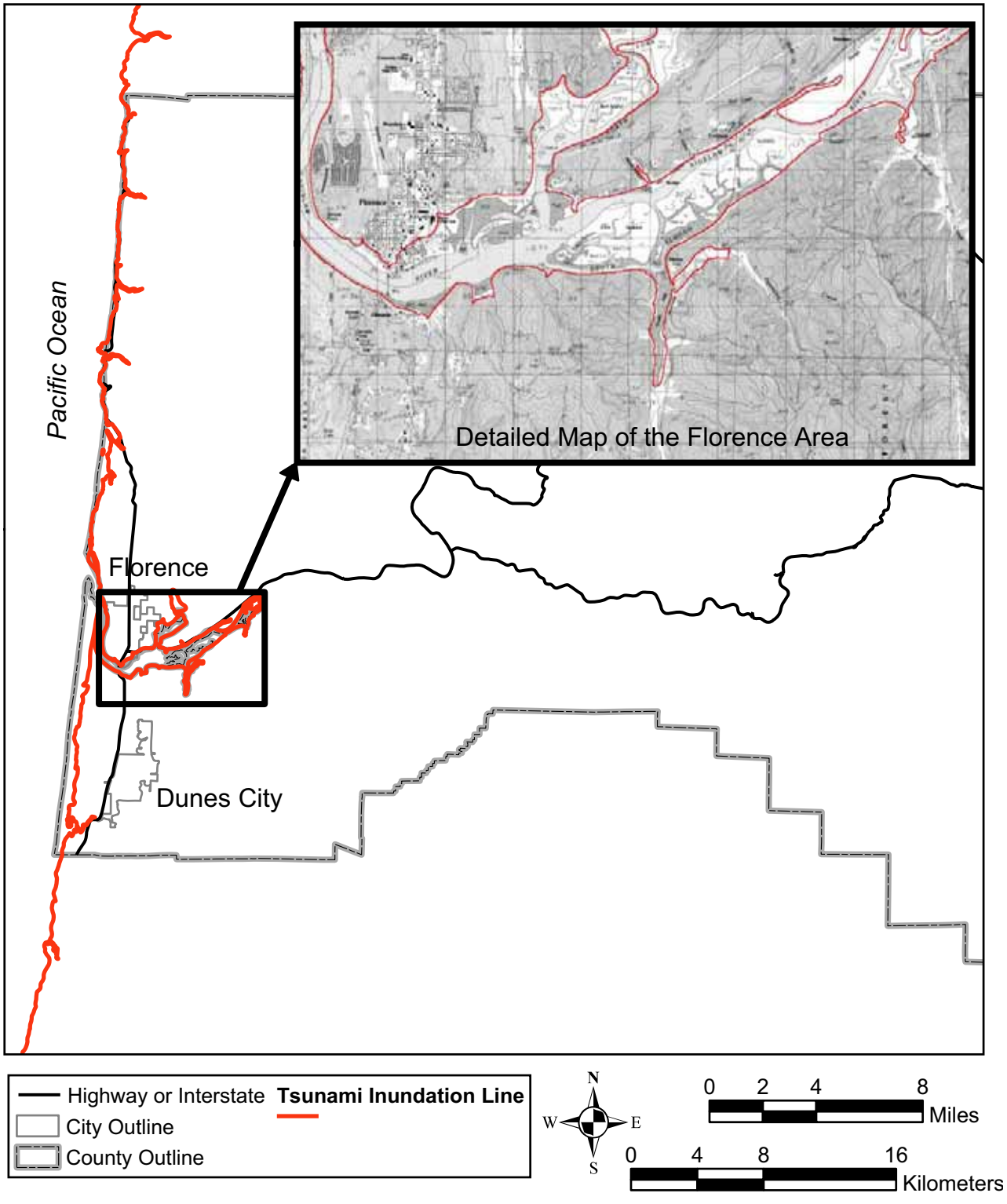

Figure 18. Tsunami inundation zone line for Lane County and the City of Florence, Oregon (modified after Priest, 1995).

Table 3. Landslide hazard class assignments based on combination of material type categories (Low, Moderate, High, and Very High) and slope gradient values.

Geologic Group (relative slope instability susceptibility)	Slope					
	0°–10°	10°–15°	15°–20°	20°–30°	30°–40°	40°+
Low (consolidated rock)	low	low	low	moderate	high	very high
Moderate (highly weathered rock and unconsolidated sediments)	moderate	moderate	moderate	high	very high	very high
High (existing landslides, landslide topography, and colluvium)	high	high	high	very high	very high	very high

of the Willamette River south of Salem are shown as higher susceptibility areas.

6.4.2 Identified Landslide Areas

Slopes that have failed in the past often remain in a weakened state, and many landslide areas tend to fail repeatedly over time. In some cases, areas that have previously failed assume rather subtle geometries, and these areas may or may not be obvious on relative hazard maps that emphasize slope (such as the earthquake-induced landslide map described in the previous subsection). Previously failed areas are nonetheless particularly important to identify, as they may pose a substantial hazard for future instability.

In this study, we extracted existing landslide polygons from the final geologic map to create the identified landslide hazard layer. This GIS compilation of landslide areas was derived from published geologic reports and existing geologic hazard studies.

We used GIS operations to select areas mapped as landslide deposits and colluvium and/or digitized the original maps to develop the database of identified landslide areas.

The current GIS layer includes more than 1,000 landslide areas (Figure 20). Some landslide areas overlap because of variations in interpretation by individual mappers. For sources in the Willamette Valley, we performed some manual editing to minimize duplication of landslide entries by selecting the most topographically accurate source. The existing information is not comprehensive, but future efforts can build on and refine the data.

6.4.3 Landslide Inventory

The regional inventory of landslides by Hofmeister (2000) incorporated information compiled by federal, state, and local data sources following the 1996-1997 storms in Oregon. The quality of the data varies considerably. This inventory is the foundation for the statewide database of landslide locations maintained by DOGAMI. The database format is easily expandable to include additional events as they are recorded. For example, the landslide data form in Appendix K can be used in conjunction with the existing inventory to efficiently gather data on future landslides. Landslide locations within the current study area from the Hofmeister (2000) study are shown in Figure 21.

Landslide inventories are valuable for tracking and monitoring historic effects, such as how many times a road cut has sloughed at one location, as well as for mitigating future effects, such as the cost effectiveness of fixing a location that sloughs every year and needs maintenance versus the cost of the yearly maintenance. Such inventories are also helpful for evaluating regional trends, calibrating existing hazards, and developing new hazard identification and mitigation tools (for examples, see Turner and Schuster [1996]). In general, the more extensive and complete the available base information, the more accurate follow-on studies can be.

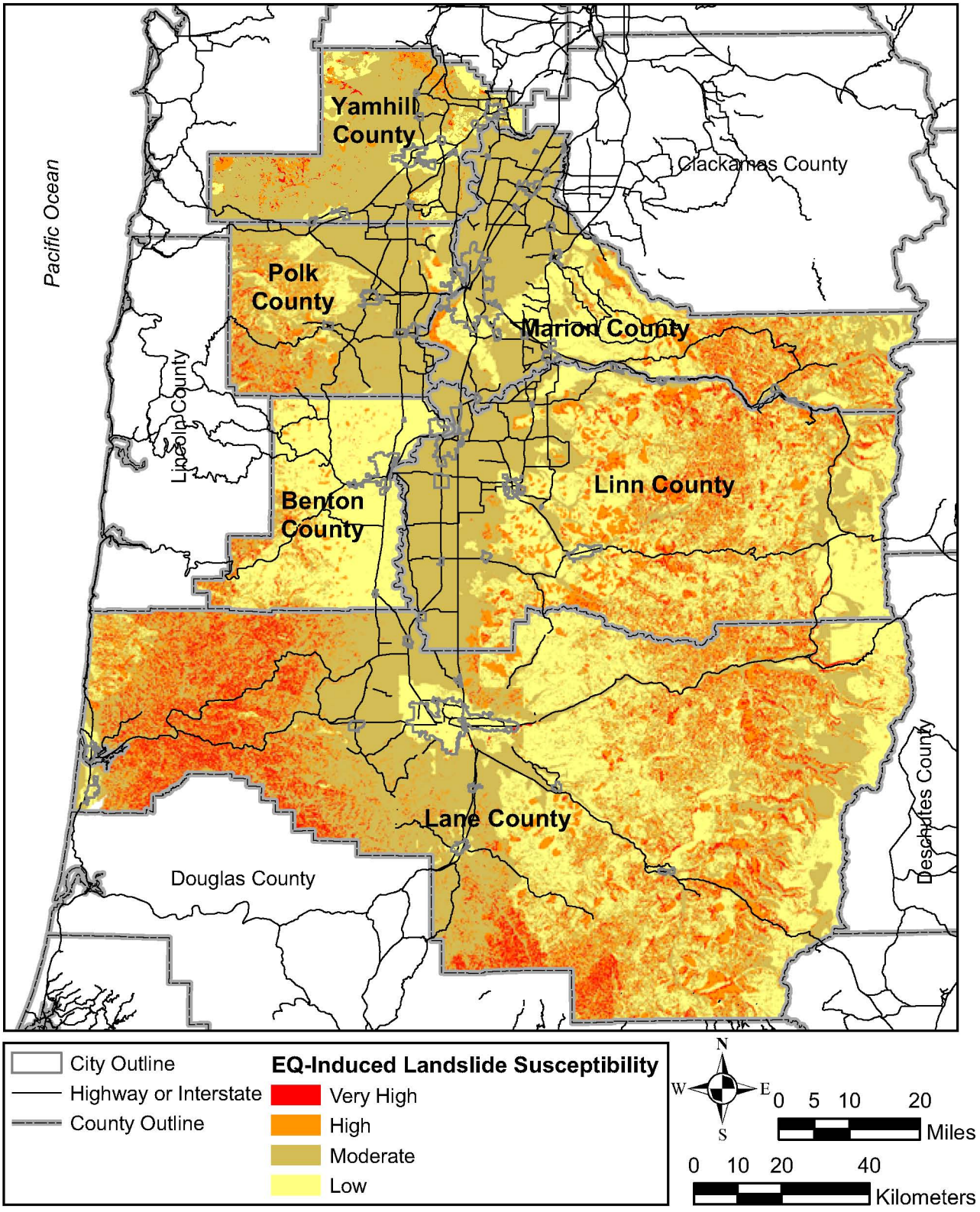

Figure 19. Earthquake-induced landslide hazard map for the study area displays the four relative hazard classes: Low, Moderate, High, and Very High. Benton County data were modified from Wang and others (2001).

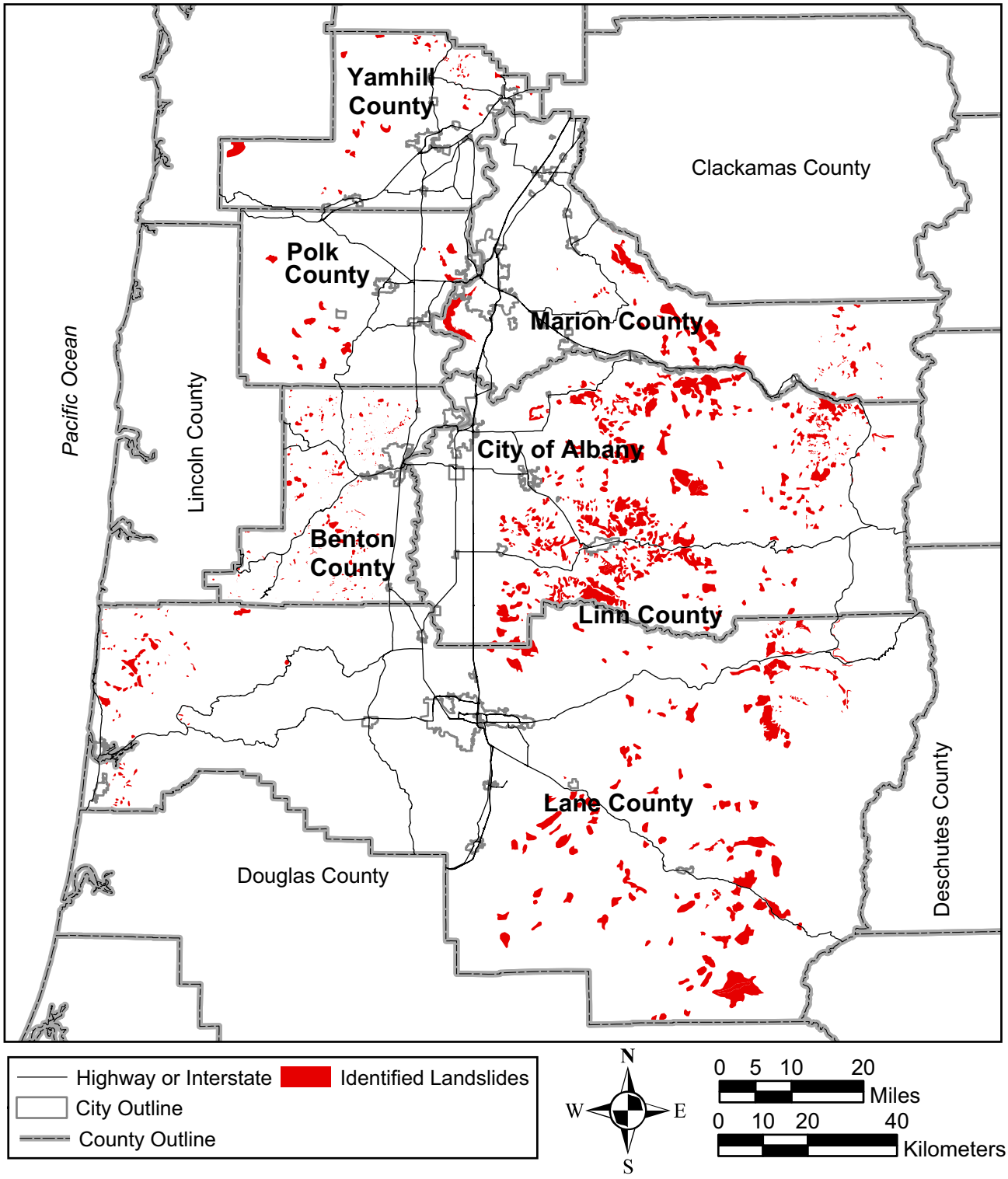

Figure 20. Identified landslides map of study area. Over 1,000 identified landslide areas are shown.

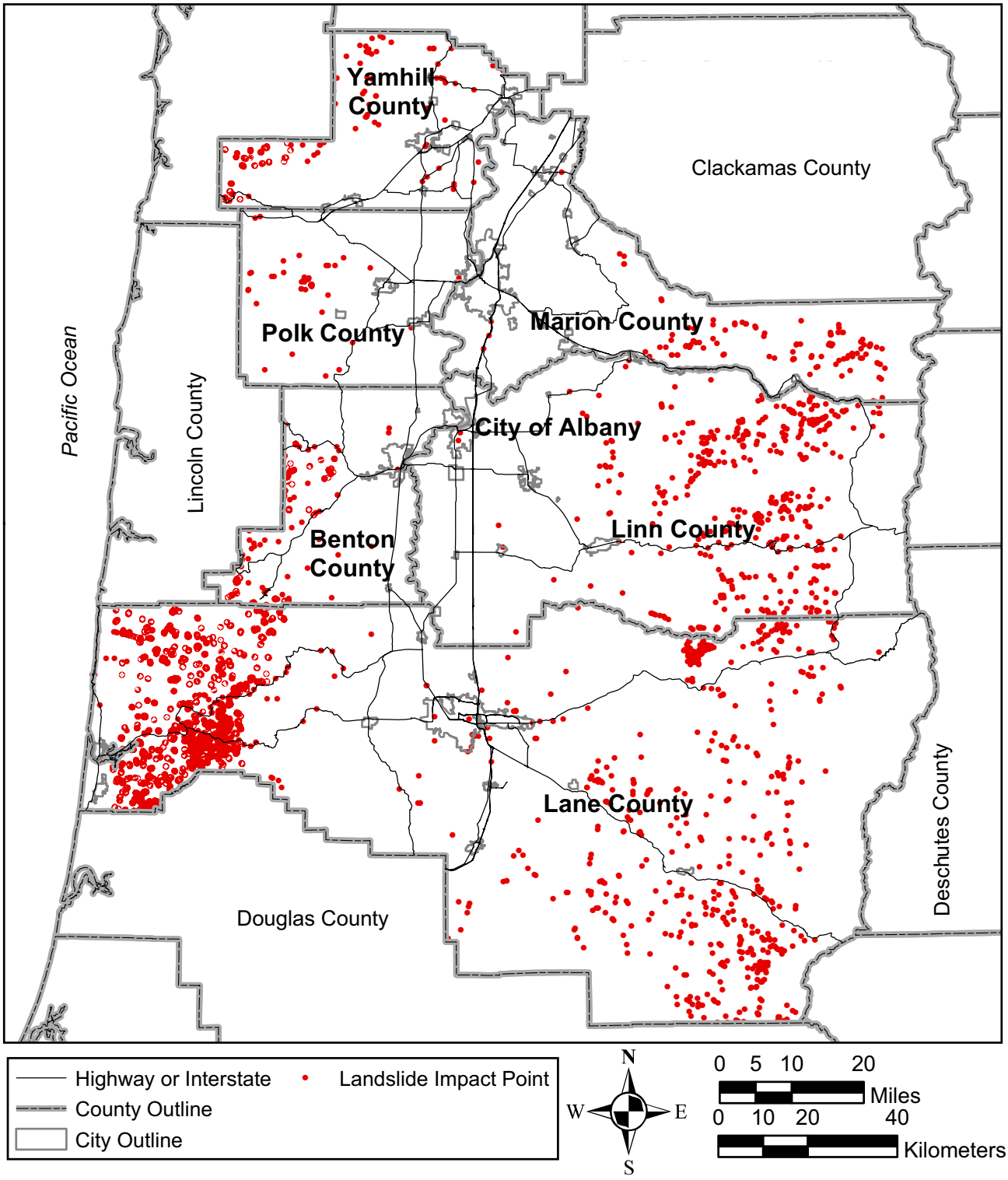

Figure 21. Landslide impact inventory from three storm events during 1996-1997. Landslide locations are mapped as points (Hofmeister, 2000).

6.4.4 Debris Flow/Rapid Moving Landslide Areas

Debris flows can originate as minor landslides and grow dramatically in size as they move down stream channels, causing tremendous destruction miles from their origins. Large debris flows can travel at velocities exceeding 50 mph and are easily capable of flattening homes, crushing cars, and taking the lives of people in their paths. In 1991 in an attempt to address the most dangerous landslide hazards more systematically, the Oregon legislature passed Senate Bill 12 (SB 12) with the overarching goal of saving lives and reducing future landslide losses.

Hofmeister and others (2002) produced a landslide hazard map showing areas where debris flows or rapidly moving landslides (RML) are possible in western Oregon. The debris flow maps were created by computer models that divide the debris flow process into three zones: 1) source area, 2) transport zone, and 3) deposition zone. An iterative process that included multiple phases of GIS screening, field data collection, inventory comparisons, and peer reviews was used to create the map (Hofmeister and others, 2002). In the final map, the three zones were combined into a single zone as shown in Figure 22.

6.5 Other Geologic Hazards

6.5.1 Volcanic Hazard Maps

In the study area the USGS defines two potentially active volcanic hazard regions, the Mount Jefferson region and the Three Sisters region (Figure 23). Numerous small volcanoes occupy areas between these regions but pose only local hazards (Walder and others, 1999). Appendix I includes the volcanic hazard maps developed by the USGS for these regions.

6.5.2 Dam Failure Maps

Throughout Oregon there are thousands of dams ranging in size and type from earthen constructions only several meters high to concrete constructions tens of meters high. Some of these dams were built before many geologic hazards such as a Cascadia Subduction Zone earthquake were identified. The National Inventory of Dams (NID) tracks 812 of these dams in Oregon, because they meet certain criteria including significant hazard potential and height (Goettel and others, 2004). Two hundred and seventy nine of these dams have a high or significant hazard (Figure 24) (Goettel and others, 2004). As previously mentioned, this hazard is related only to the impact if a dam fails, not to dam safety level or likelihood to fail. In order to assess the risk from dam failure, communities should acquire or produce inundation zone maps. An example of an inundation zone map from outside the study area is shown in Figure 25.

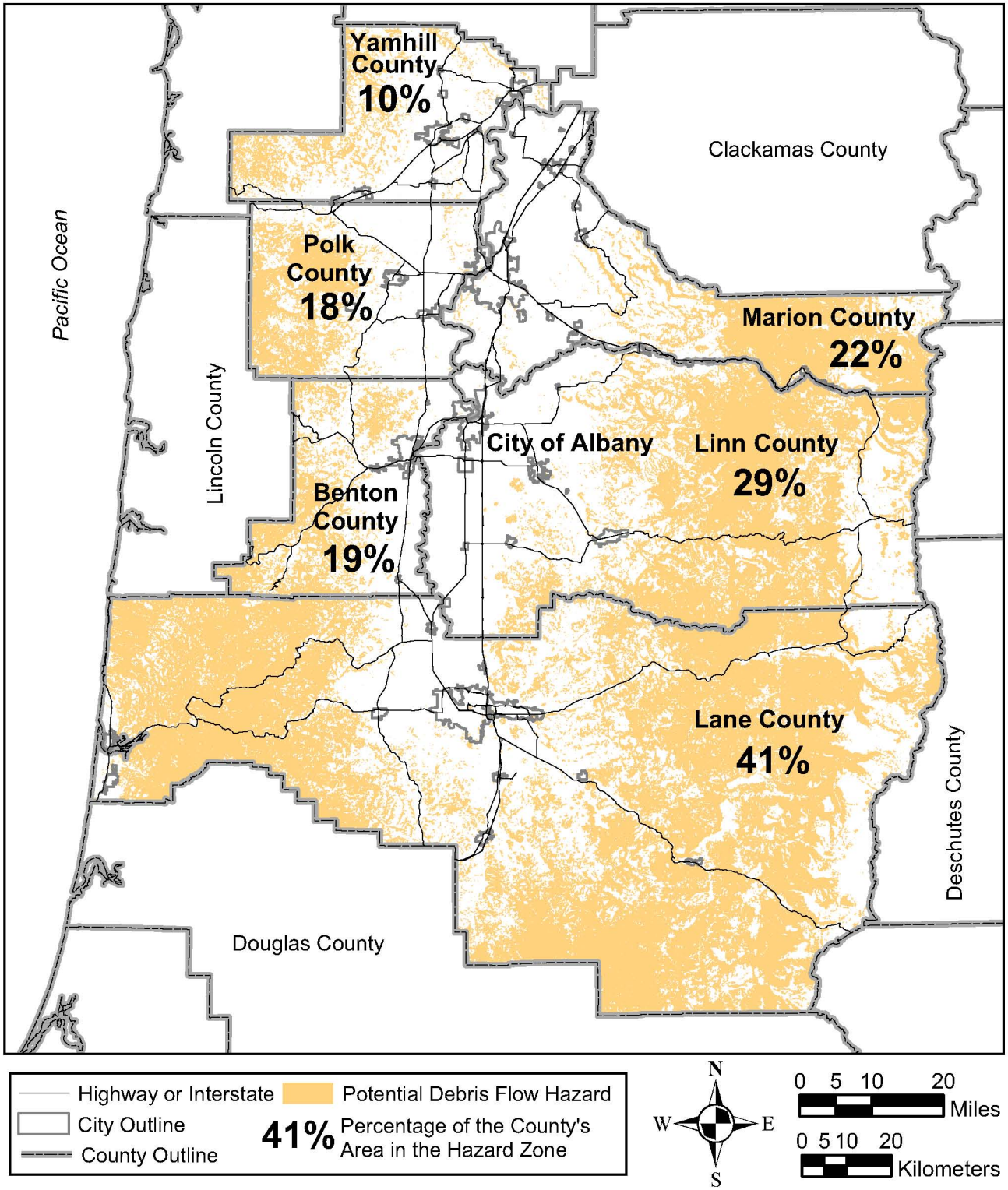

Figure 22. Debris flow ("rapidly moving landslide") hazard map displaying areas in the hazard zone and percentage of county area in the hazard zone (Hofmeister and others, 2002).

Figure 23. Aerial view looking north toward Three Sisters (left) and Broken Top (right) (Walder and others, 1999).

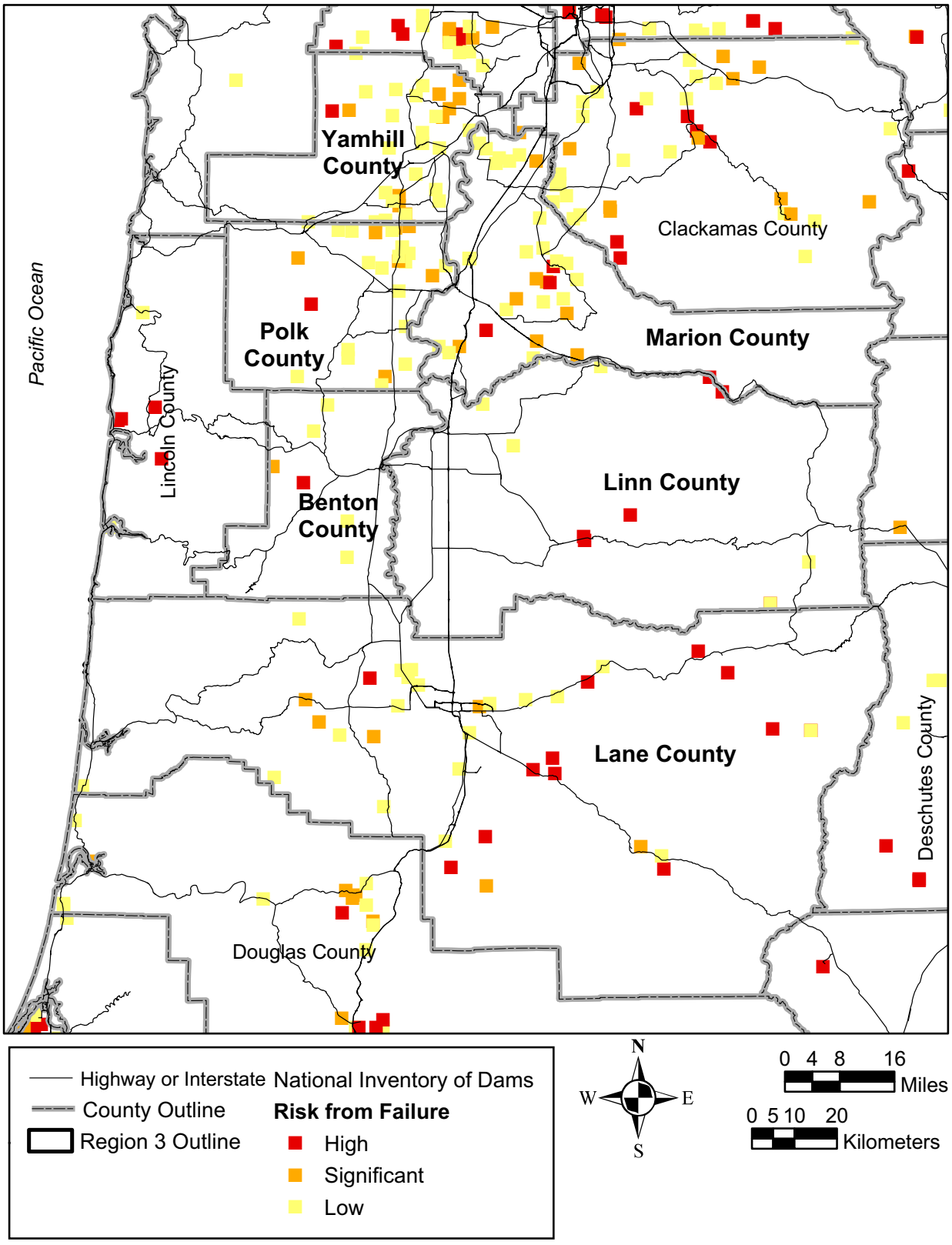

Figure 24. Map of National Inventory of Dams (NID) dams with relative levels of related risk from impact if dams were to fail (U.S. Army Corps of Engineers, 2005).

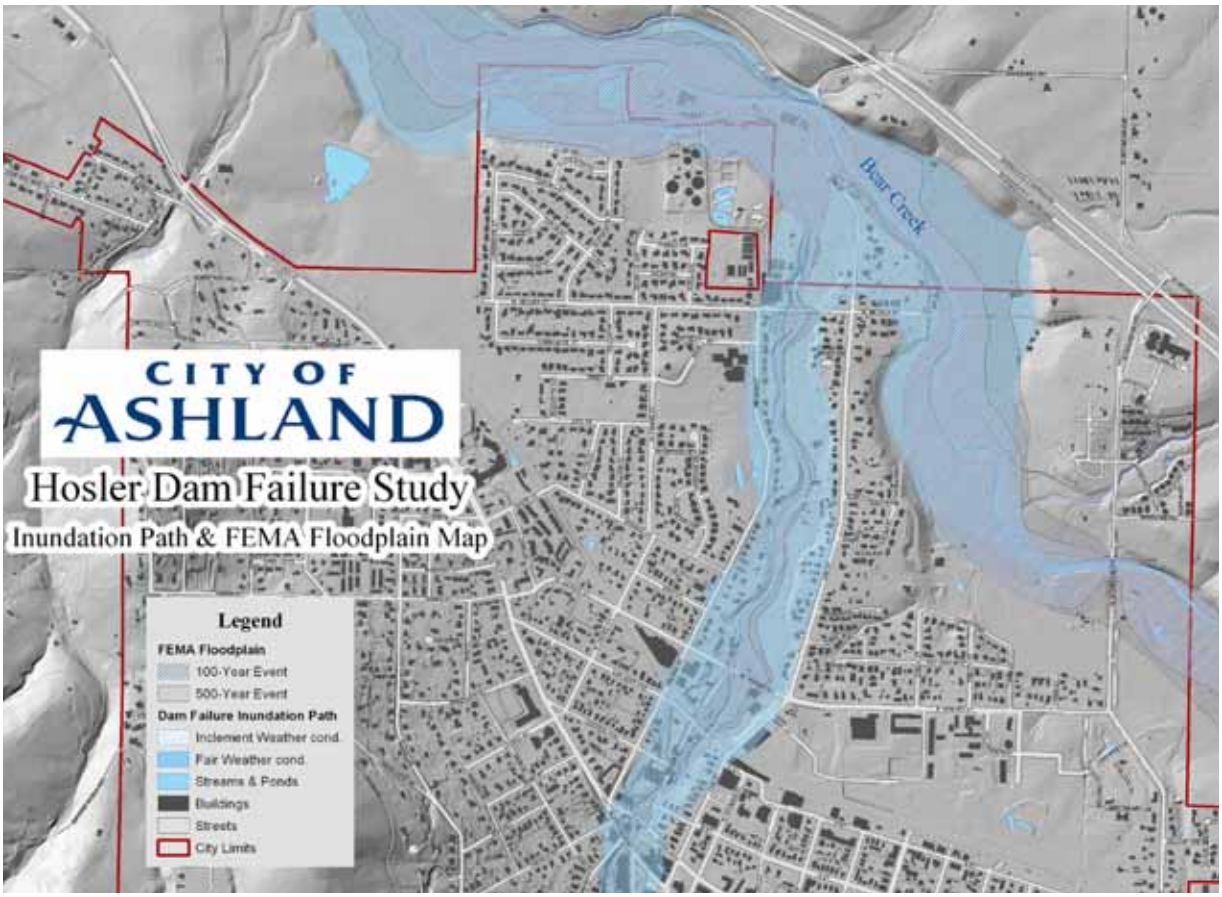

Figure 25. Example of a dam failure inundation map for the City of Ashland, Oregon (City of Ashland, 2005).

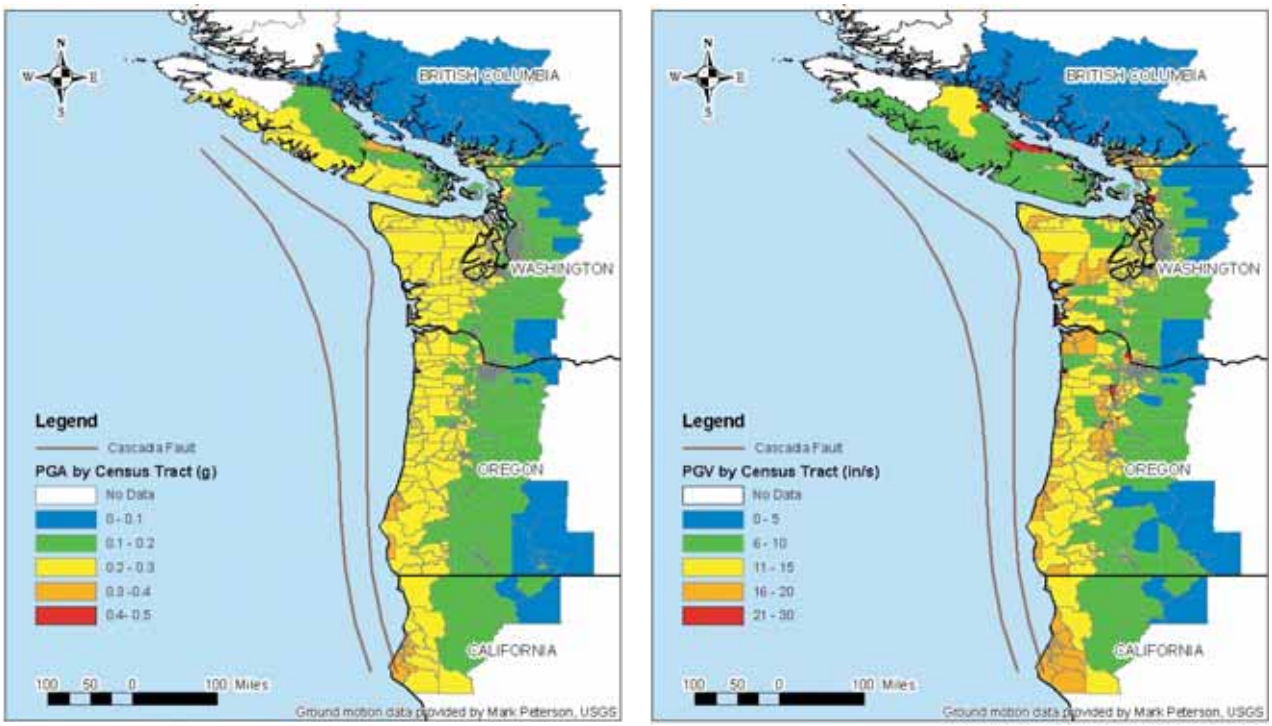

Figure 26. (left) Peak ground accelerations (PGA) and (right) peak ground velocities (PGV) on rock for the Cascadia Region Earthquake Workshop (CREW) magnitude 9.0 Cascadia Subduction Zone scenario. (CREW, 2003).

6.6 Map Limitations and Recommended Future Improvements

We developed the countywide earthquake hazards and landslide hazard maps with the best data available and the most appropriate models allowed by project funding. Several limitations are worth noting and underscore that any relative hazard map is generally useful for regional applications but should not be used as an alternative to site-specific studies in critical areas.

1. Although it is possible to check for errors in the GIS and database operations, it is not feasible to verify completely the original data on which the analyses are based. Geologic data in less populated eastern portions of the counties were particularly limited in terms of scale. For example, the 500,000-scale geologic map of the state was used in some locations, and the available GIS layers were poorly georeferenced. We manually edited the layers to improve some areas, but time constraints prohibited extensive modifications.
2. We developed hazard layers from original sources that vary in scale, methods of development, and quality. Changes subsequent to the period of the original mapping — such as advancement of rock quarry boundaries, large-scale earthwork projects, large landfills, and other land modifications — could affect the hazard ratings in some areas. Land modification is not expected to be a significant source of error, but land modifications can be important locally in some areas.
3. We assigned hazard classes on the basis of regional data with substantial scatter. We selected the most representative values, but geologic materials do vary regionally and locally. Site-specific geologic features, such as the presence of daylighting discontinuities, unfavorably dipping bedding planes, seams of local weakness, and other causes of localized instability cannot realistically be determined on a regional basis for each cell. Yet these can be critical factors for particular areas.
4. We neither collected nor analyzed any new data to create these maps. Therefore these maps are snapshot views of the current data.

Because of these limitations and because the hazard zones are based on limited geologic data as described in this report, these maps are intended for regional purposes only and cannot replace site-specific investigations. However, the relative hazard maps can serve as useful tools for estimating the regional effects of future earthquake and landslide events.

6.6.1 Recommendations for Improvements (Action Items)

To improve the existing hazard maps and data, action items are provided in Appendix J. These action items range from identification of individual school buildings that have a high risk of collapse in an earthquake to identification of landslide hazard areas over large regions of the state. Table 4 lists the three multi-hazard action items:

Table 4. Multi-hazard action items.

Action Item	Goal	Partners
Identify and pursue funding opportunities to implement mitigation actions.	The switch from planning to implementation is the step that begins the reduction of risk.	Form partnerships with city, other county, and state agencies. Use these partnerships to apply for federal and local (local bonds, measures) mitigation grants.
Integrate the hazard data into planning ordinances and regulatory documents and programs.	Without ordinances and regulations, the hazard data are used by only few, instead of by all.	Work with local and regional governments.
Develop education programs aimed at mitigating the risk posed by hazards.	Education of the potential hazard and risk are sometimes the best way to reduce the risk.	Work with local and regional governments. Use internet websites, local fairs, news articles, brochures, etc to get the data to the public.

7.0 EARTHQUAKE DAMAGE AND LOSS MODELING

The second major component of this study was to perform earthquake-induced damage and loss modeling for each community partner involved in the Region 3 PDM Project: Yamhill, Marion, Polk, Benton, Linn, and Lane Counties and the City of Albany, Oregon. The general purpose of damage and loss estimation is to evaluate resource requirements for earthquake effects and to identify areas where planning and mitigation can be implemented most effectively.

The state of the science in earthquake damage and loss estimation has improved dramatically over the last several years, and new tools allow for relatively quick and reasonably accurate regional loss estimation. One such tool is the HAZUS-MH computer program developed by the Federal Emergency Management Agency (FEMA), the National Institute of Building Sciences (NIBS), and a host of other public and private partners (FEMA, 2003, 2005). The HAZUS-MH software can be used to model a variety of earthquake scenarios and to estimate regional damages such as building damage, lifeline damage (roads, utilities), and injuries.

A number of default databases are included with the HAZUS-MH program. Most data are based on national-scale information that often does not accurately reflect local conditions. To better account for local variability the software is designed to incorporate user-specific updates to the data inputs (FEMA, 2003). In this study, we incorporated the updated regional hazard maps presented in the preceding sections. With the HAZUS-MH study region geologic hazard data updated, a local crustal earthquake scenario and a Cascadia subduction zone scenario for each community were input (Table 5) and analyzed. The results are summarized in Table 6 and Appendices A–G.

Table 5. Earthquake scenarios input for HAZUS-MH analysis.

Community	Crustal Scenario	Magnitude	Subduction Zone Scenario	Magnitude
Benton County	Corvallis Fault	6.5	Cascadia	9.0
City of Albany	Mill Creek Fault	6.7	Cascadia	9.0
Lane County	Arbitrary "Eugene" Fault	6.5	Cascadia	9.0
Linn County	Mill Creek Fault	6.7	Cascadia	9.0
Marion County	Mt. Angel Fault	6.9	Cascadia	9.0
Polk County	Mill Creek Fault	6.7	Cascadia	9.0
Yamhill County	Newberg Fault	6.8	Cascadia	9.0

Table 6. Summary of estimated building related damage/losses from HAZUS-MH analysis.

County	Scenario	Estimated Moderately to Completely Damaged Buildings		Total Building-Related Losses (includes estimates caused by business interruption) (billions of dollars)
		Number of Buildings	Percent of Total Buildings	
Yamhill	Crustal / Cascadia	13,600 / 9,500	50% / 35%	1.5 / 1.2
Polk	Crustal / Cascadia	4,100 / 6,100	20% / 29%	0.4 / 0.6
Marion	Crustal / Cascadia	37,400 / 21,700	43% / 25%	3.9 / 2.6
Benton	Crustal / Cascadia	7,700 / 8,100	31% / 32%	0.8 / 1.1
Lane	Crustal / Cascadia	28,400 / 32,500	25% / 29%	3.4 / 5.0
Linn	Crustal / Cascadia	12,400 / 10,300	34% / 29%	1.3 / 1.2
Total	Crustal / Cascadia	NA / 88,200	—	NA / 11.7

NA: It is very unlikely that these events would happen at same time; therefore the values were not totaled.

7.1 Improvements to the HAZUS-MH Base Model

7.1.1 HAZUS-MH Compared to HAZUS-99

The HAZUS-MH (FEMA, 2003b) model was improved from the HAZUS-99 model by the addition of data and improvements to the methodology including:

- New 2002 aggregated data for square footage, building count, building exposure, content exposure, and demographics
- New site-specific inventory data (2000 or later)
- New 2002 USGS probabilistic ground-shaking maps and new USGS attenuation functions

7.1.2 Addition of Relative Earthquake Hazard Maps

We used the relative earthquake hazard maps described in section 6 to update the HAZUS-MH study region. To input the maps into HAZUS-MH, specific formats and classifications are required. For ground-shaking amplification hazard, we incorporated GIS polygons into HAZUS-MH by assigning the hazard polygons as shown below.

Amplification Class	Amplification Susceptibility	HAZUS-MH Input
a	very low	a
b	low	b
c	moderate	c
d	high	d
e	very high	e
f	site specific	f

For liquefaction, the layer hazard classes were assigned as shown in below.

Liquefaction Class	Liquefaction Susceptibility	HAZUS-MH Input
a	rare	0
b	very low	1
c	low	2
d	moderate	3
e	high	4
f	very high	5

For landslides, we tested a number of options for incorporating the detailed hazard map information into the HAZUS-MH program. For landslides, we broke down the relative zones into only four classes; HAZUS-MH classes 0, 2, 3, 5, 6, 8, and 9 were not used. We ended up with classes as shown below:

Landslide Class	Landslide Susceptibility	HAZUS-MH Input
—	—	0*
low	low	1
—	—	2*
—	—	3*
moderate	moderate	4
—	—	5*
—	—	6*
high	high	7
—	—	8*
—	—	9*
very high	very high	10

*HAZUS-MH class not used for input.

7.2 Earthquake Scenarios

The updated HAZUS-MH regions included with this report allow one to run any number of plausible earthquake scenarios in the study area. To test the model and to provide some examples, we have included results from two sample scenarios for each community:

1. Crustal earthquake with varying magnitude between 6.5 and 6.9
2. Subduction zone earthquake with magnitude 9.0 developed by the Cascadia Region Earthquake Workgroup (CREW, 2003).

Appendices A–G have details about the earthquake scenarios for each community. Table 5 summarizes the earthquake scenarios run as examples for this study.

The crustal earthquake event was chosen by examination of USGS data and data in the Geomatrix Consultants, Inc. (1995) report prepared for the Oregon Department of Transportation. A likely worst-case scenario was selected in each case. For Lane County, because no potentially active fault within or adjacent to the population center (Eugene-Springfield) has been identified yet, an arbitrary fault was developed (details are included in Appendix C).

For the Cascadia Subduction Zone earthquake scenario, we used the "user-defined event" option within HAZUS-MH to incorporate ground motion maps developed by CREW to model a magnitude 9.0 earthquake. Ground motion data provided by the U.S. Geological Survey are the basis for the CREW maps. Figure 26 shows CREW regional peak ground acceleration (PGA) and peak ground velocity (PGV) maps (CREW, 2003). The CREW earthquake scenario required input of four sets of GIS files that are included within the HAZUS-MH study region: regional peak ground acceleration (PGA), peak ground velocity (PGV), and the spectral velocity at 0.3 and 1.0 (CREW, 2003).

Two factors should be used to assess the risk posed by the scenarios: the amount of expected damage and the relative likelihood of an earthquake on these two faults. In the last two decades, the Cascadia Subduction Zone has been extensively studied; the average recurrence interval for this event is expected to be about 500 years. The recurrence interval for the crustal faults is far less constrained (Wang and others, 2001).

Another difference between the two earthquake scenarios is duration of shaking. Although the Cascadia Subduction Zone earthquake will not produce shaking as violent as a large-magnitude crustal earthquake in the near field, the duration of strong shaking will be much longer. Cascadia Subduction Zone earthquake shaking may last longer than 5 minutes, whereas strong shaking for crustal earthquakes may last 20–30 seconds. The 2004 Sumatra Subduction Zone Earthquake triggered shaking that lasted between 7 and 10 minutes (Park and others, 2005). Due to some limited scientific and engineering constraints on the effect of the longer duration Cascadia Subduction Zone shaking, HAZUS-MH damage estimates for this event have large uncertainty.

7.3 Summary of HAZUS-MH Results

Global summary results from running the model for these two earthquake scenarios are provided in Appendices A–G. The results from both models show that either earthquake would result in significant losses in all communities of the study. Results of the two scenarios for related damage/losses are compared in Table 6 and Table 7.

Table 7 shows roughly 1,000 casualties and 13,000 injured people would result in the study area from a Cascadia event. It also indicates that roughly 6,000 people would need shelter after a Cascadia event.

$12.5 billion in total economic losses from a Cascadia event is estimated. But, the total economic loss values are most likely underestimates due to the low quality and quantity of the input data, especially the lifeline data. Limitations of the data are discussed in more detail in section 7.5 of this report.

Table 8 shows a comparison of estimated available hospital beds in the study area before and after a Cascadia earthquake. HAZUS-MH estimated roughly 1,000 beds would be available the day after the earthquake and roughly 3,500 people would require hospitalization the day after.

Table 7. Estimated social impact of a crustal or Cascadia Subduction Zone earthquake from HAZUS-MH analysis.*

County	Earthquake Scenario	Fatalities During Late Afternoon Business Hours	Injuries from Minor to Life Threatening	Households Displaced	People Needing Shelter
Yamhill	Crustal / Cascadia	80 / 90	1,260 / 1,380	4,250 / 3,080	1,000 / 750
Polk	Crustal / Cascadia	20 / 50	280 / 720	1,410 / 1,820	360 / 460
Marion	Crustal / Cascadia	240 / 220	3,720 / 3,170	10,700 / 5,780	2,730 / 1,470
Benton	Crustal / Cascadia	40 / 120	590 / 1,560	1,750 / 2,370	500 / 660
Lane	Crustal / Cascadia	130 / 370	2,080 / 5,200	7,710 / 7,660	2,000 / 2,000
Linn	Crustal / Cascadia	70 / 90	1,120 / 1,290	3,680 / 2,560	920 / 650
Total	Crustal / Cascadia	NA / 940	NA / 13,320	NA / 23,270	NA / 5,990

*See Appendices A–G for detailed scenario input for each county.

NA: It is very unlikely that these events would happen at same time, and therefore the values were not totaled.

Table 8. Comparison of estimated hospital beds before and after a Cascadia Subduction Zone earthquake.

	Before Earthquake			After Cascadia Earthquake		
County	Number of Hospitals	Available Hospital Beds (approximate)	Average Beds per Hospital	Number of Hospitals Likely Functional Day After	Average Beds Available the Day After	Injuries Requiring Hospitalization
Benton	1	130	130	1	130	420
Lane	4	580	145	1	145	1350
Linn	1	70	70	1	70	340
Marion	5	1070	214	3	642	810
Polk	1	40	40	0	0	190
Yamhill	2	100	50	0	0	360
Total	14	1990	142	6	987	3470

7.4 Comparison of Results with Previous Studies

It is worth comparing the results of the current study with previous estimates of earthquake losses, including the statewide seismic risk assessment conducted by Wang and Clark (1999) and Wang (1998). In Marion County, for example, Wang and Clark (1999) used HAZUS-97 and its data, which indicated a magnitude 8.5 Cascadia Subduction Zone earthquake could cause nine fatalities, 1,241 displaced households, and $13 million in highway damage. Estimates for this study's scenario using HAZUS-MH and its data (2000 census data) for a magnitude 9.0 Cascadia Subduction Zone were 218 fatalities, 5,787 displaced households, and $127 million in highway damage. These increases in losses are mainly attributed to the addition of user-specified hazard layers, including liquefaction and landslides, the updated inventory data from the 2000 census, and a higher magnitude earthquake.

A second comparison worth looking at is between DOGAMI's Open-File Report O-01-05, *Preliminary Earthquake Hazard and Risk Assessment, Benton County* (Wang and others, 2001) and this study. The 2001 study used HAZUS-99 (FEMA, 1999) and augmented the default data with field survey data. The field survey resulted in, for example, a 22 percent improvement in single-family residential building area

data, an improvement in Oregon State University campus building data, and a 4 percent improvement in commercial building data. The estimates using the HAZUS-99 with the field data and a crustal scenario (Corvallis Fault) resulted in 0 fatalities, 695 displaced households, and $707 million in building damage. The estimates for this study using HAZUS-MH without the updated field survey data are 38 fatalities, 1,755 displaced households, and $762 million in building damage. These changes are mainly attributed to the 2002 aggregated data for square footage, building count, building exposure, content exposure, and demographics updated in the HAZUS-MH model and the updated program functions.

The HAZUS-MH study regions for each community in this study are included on the publication CD, so that users can run a variety of default and custom scenarios as well as evaluate probabilistic losses. This allows users a maximum amount of flexibility.

7.5 Uncertainties in Damage and Loss Estimation

Any city, county, or region studied will have huge varieties of population type and density, transportation and lifelines, structures, and type and level of hazard. Due to this complexity and uncertainties inherent in any estimation methodology (FEMA, 2003b), readers should bear in mind the limits of the estimates given here.

7.5.1 HAZUS-MH Modeling Limitations

Although the HAZUS-MH software allows us to analyze complex and extensive regional earthquake scenarios, which result in statistically reasonable loss estimates, it is important to note the potential uncertainties associated with this type of modeling. These uncertainties arise from such factors as incomplete scientific knowledge concerning earthquakes and their effects on structures, incomplete or inaccurate inventories of the built environment/demographic/economic parameters, and other simplifications and approximations necessary for comprehensive analyses (FEMA, 2003b). Some examples of these uncertainties include the spatial variability of ground motions, the averaged building data by census tracts, and variations or errors in empirically derived algorithms implemented within the program (FEMA, 1999). These factors all limit the ability to calculate precisely the regional damages and losses and therefore "can result in a range of uncertainty in loss estimates produced by the HAZUS-MH Earthquake Model, possibly *at best* a factor of two or more" (FEMA, 2003b, p. 6).

7.5.2 Specific HAZUS-MH Modeling Limitations

During the damage and loss modeling using HAZUS-MH, we noticed several results that are consistently incorrect or underestimated across all counties. Lifeline data (transportation and utilities) appear to be the least reliable, which is not surprising as these data are the most difficult to collect and analyze. An example of the inaccuracy of the data can be seen in the Lane County Cascadia Subduction Zone scenario results shown below:

Railways	0% with at least moderate damage
Highway Segments	0% with at least moderate damage
Natural Gas Facilities	0% with at least moderate damage
Electrical Power Facilities	0% with at least moderate damage
Electric Power Performance	0 households without service the day after

We also noticed the results related to critical facilities were underestimated across all counties. The Oregon Department of Geology and Mineral Industries is currently performing a statewide study of critical facilities, which will improve the portion of the data in HAZUS-MH.

8.0 POTENTIAL USES OF THE STUDY DATA

The primary purpose of this study's consolidation of geologic hazard maps and loss estimation tools is to enable follow-on risk assessments and to focus resource allocation toward vulnerable areas. In general, the relative hazard maps should serve as useful tools for differentiating areas of higher and lower hazards. This spatial information is basic to emergency and land-use applications, and the following sections provide an overview of some common uses of the relative hazard maps and the earthquake damage and loss data.

With the risk assessment (damage and loss) estimate results, one can begin to:

- Identify vulnerable areas that may require planning considerations
- Assess the level of readiness and preparedness to deal with a disaster before disaster occurs
- Estimate potential losses from specific hazard events (before or after a disaster hits)
- Decide how to allocate resources for most effective and efficient response and recovery
- Prioritize mitigation measures that need to be implemented to reduce future losses

An example of preparedness and post-event community recovery can be examined by looking at the Marion County crustal earthquake scenario results. The data indicate ~60% of the fire stations will be functional the day after the modeled event and 18 fires will be ignited. For this scenario, one can see the need to mitigate the 40% of the fire stations that are nonfunctional so they do not become the weak link in the community's response and recovery from a disaster.

The items discussed below are just a few potential applications. It is likely that individual communities will find unique and new applications to suit particular needs.

8.1 Emergency management applications

A valuable use of the maps and loss estimation products is as an aid in emergency management activities such as development and refinement of emergency response plans, public outreach activities, selection of appropriate safe-haven sites, hazard response drills, and estimation of resource impacts for various earthquake hazard scenarios (Spangle Associates, 1998). An example of useful output data to an emergency management application is the debris generation estimate. In Marion County for a crustal scenario, HAZUS-MH estimated roughly 1 million tons of debris would be generated and at 25 tons/dump truck load would result in the need for 40,000 truck loads for debris removal. These data can be used by Marion County to prepare a post-disaster recovery plan that might involve the temporary rental of trucks and additional landfill space for the generated debris.

In related applications, communities and others can use the landslide and liquefaction hazard maps to identify infrastructure that is more or less likely to be damaged by major earthquakes and/or landslide-producing storm events. For example, by combining the hazard maps with transportation layers, potential road blockages can be identified and alternative corridors can be located. Similarly, the hazard maps can be combined with other information (such as the locations of hazardous waste facilities) to evaluate potential effects and to plan for emergency response.

HAZUS-MH inputs and outputs are also tailored to address specific emergency management and emergency planning needs. HAZUS-MH results provide estimates for various earthquake scenarios of the number of displaced individuals needing shelter, medical facility needs (for minor and major injuries), locations to concentrate rescue and recovery vehicles to limit damages, and so on. These estimates can be compared with information on currently available facilities and resources within the county.

8.2 Land-use planning, zoning, and regulations

Common applications of the study outputs in the realm of land-use planning, zoning, and regulations include input to comprehensive planning and the development of hazard ordinances. We reiterate that the relative hazard maps are not appropriate for site-specific evaluations, but the maps are valuable for regional screening for hazards and the selection of appropriate areas on which to focus further site-specific studies.

The landslide layers are particularly suitable for incorporation into county and city hillside development ordinances. The liquefaction hazard map can be used for regional screening of locations where further review may be warranted, and the information could be integrated into relevant local ordinances. The amplification hazard map is not as well suited for ordinance implementations because site amplification can generally be accounted for in standard infrastructure design phases. Therefore, amplification hazards are typically addressed by the adoption and enforcement of building code standards (Spangle Associates, 1998).

8.3 Evaluations of lifelines and other regionally distributed infrastructure

"Lifelines" is a general term used to refer to critical transportation and utility infrastructure, including roads and highways, railroads, airports, bridges, overpasses and underpasses, natural gas pipelines, electric lines, and water distribution systems. Many lifelines are characterized by components that are dispersed over broad geographic areas that often require regional (as opposed to site-specific) risk assessments. The hazard maps presented in this report can be useful for estimating and mitigating damage to lifelines.

HAZUS-MH includes regional risk assessment algorithms for lifelines, but assessments can also be made outside the HAZUS-MH program and are not limited specifically to lifeline components. Any number of geographically dispersed infrastructure components can be evaluated by identifying the intersections of hazard zones with infrastructure inventories. It is relatively common in Oregon to incorporate regional hazard maps into the planning stages for lifelines such as natural gas pipelines and water distribution systems, and it is also appropriate in some cases to use the relative hazard maps to screen the planning process of larger developments. Comparing the maps to various development plans can provide valuable feedback on locations that may be worth avoiding (higher hazard areas) and locations where a denser concentration of structures may be preferable (in lower hazard areas).

8.4 Earthquake rehabilitation programs

While it is usually more cost effective to take steps toward mitigation before development occurs, the reality is that there are a lot of existing buildings and other infrastructure components built prior to the incorporation of earthquake design into the codes. With some existing infrastructure, it makes sense to upgrade (or "rehabilitate") to current earthquake design standards.

Critical and essential facilities including fire, hospital, police stations, emergency centers, and school buildings are particularly important to the community and, ideally, should be designed to withstand earthquake shaking. These buildings are catalogued in this study and are incorporated into the updated HAZUS-MH building database and study region on this CD-ROM. Using this compiled information, essential facilities can be more efficiently evaluated and prioritized for earthquake rehabilitation (by such methods as benefit-cost analyses).

8.5 Ongoing data consolidation efforts

The information included in this study is a substantial improvement upon previously available earthquake and landslide hazard information for each community. It is, however, based on data sources and evaluation techniques that will improve with time and attention. As reliable new information becomes available, we encourage county agencies and other users of this information to update the data and maps provided in this study.

With the landslide hazard data, in particular, the GIS layers for identified landslide areas and the landslide impact inventory can serve as an excellent starting point, but we encourage county agencies and other users to build on the data by incorporating any additional information that becomes available. We also hope that specific inventory efforts will be conducted to add to the available information base.

Similarly, the HAZUS-MH study regions should be updated with additional local information. We focused specifically on the hazard map parts of HAZUS-MH in this study, but many other default files in HAZUS-MH can be updated to take advantage of the many additional modeling capabilities within the program. For example, dam-break flood hazards can be evaluated using HAZUS-MH if a properly formatted dam inventory is developed. Similarly, other inventory files and other parameters (e.g., local economic variables) used by HAZUS-MH can be updated wherever and whenever more accurate local information is available for input.

These examples are just a few of many potential applications that can build on the results from this study. More information on these and other applications can be found in publications by Spangle Associates (1998), FEMA (2003b), and Turner and Schuster (1996).

9.0 ACKNOWLEDGEMENTS

Funding for this project was provided by FEMA through Pre-disaster Mitigation Award EMS-2004-PC-0002, with matching funds from the State of Oregon. The report was reviewed by Carol Hasenberg from Portland State University and Steve Dickinson from Oregon State University. We are very grateful to these individuals for their generous assistance. We thank Andre LeDuc and Krista Mitchell at Oregon Natural Hazards Workgroup and Dennis Sigrist at Oregon Emergency Management. We would also like to thank all the staff at county and city agencies who worked on the natural hazard mitigation plans. These include Mark Fancey and Judith Ingram Moore (Mid-Willamette Valley Council of Governments), Bob Maca (Yamhill County), Dean Bender (Polk County), John Vanderzanden (Marion County), Mike Morrow (Benton County), Linda Cook (Lane County), Robert Wheeldon and Jim Howell (Linn County), and Darrel Tedisch and Kevin Kreitman (City of Albany). Finally, we would like to thank DOGAMI staff, especially Paul Staub, Neva Beck, Rudie Watzig, and Ian Madin.

10.0 REFERENCES

Note: Numbers in parentheses after some references correspond to reference map number labels in Figure H-2 in Appendix H. Table H-1 lists all references in reference ID order.

Allison, I. S., 1953, Geology of the Albany [15'] quadrangle, Oregon: Oregon Department of Geology and Mineral Industries Bulletin B-37, 18 p., 1 plate. **(3)**

Allison, I. S., and Felts, W. M., 1956, Reconnaissance geologic map of the Lebanon [15'] quadrangle, Oregon: Oregon Department of Geology and Mineral Industries Quadrangle Map QM-5, 1 plate. **(36)**

Atwater, B. F., 1987, Evidence for great Holocene earthquakes along the outer coast of Washington state: Science, v. 236, p. 942–944.

Atwater, B. F., and Hemphill-Haley, E., 1997, Recurrence intervals for great earthquakes of the past 3,500 years at northeastern Willapa Bay, Washington: U.S. Geological Survey Professional Paper 1576, 108 p.

Baldwin, E. M., 1956, Geologic map of the lower Siuslaw River area, Oregon: U.S. Geological Survey Oil and Gas Investigations Map OM-186, 1 plate. **(31)**

Baldwin, E. M., 1964, Geology of the Dallas and Valsetz [15′] quadrangles, Oregon (revised ed.): Oregon Department of Geology and Mineral Industries Bulletin B-35, 56 p., 3 plates. **(2)**

Baldwin, E. M., 1974, Eocene stratigraphy of southwestern Oregon: Oregon Department of Geology and Mineral Industries Bulletin B-83, 40 p., 1 plate. **(33)**

Beaulieu, J. D., Hughes, P. W., and Mathoit, R. K., 1974, Environmental geology of western Linn County, Oregon: Oregon Department of Geology and Mineral Industries Bulletin 84, 117 p., 22 plates. **(6)**

Bela, J. L., 1979, Geologic hazards of eastern Benton County, Oregon: Oregon Department of Geology and Mineral Industries Bulletin B-98, 122 p., 5 plates. **(8)**

Bela, J. L., 1981, Geologic map of the Rickreall and Salem West [7.5′] quadrangles, Oregon; Geologic map of the Monmouth and Sidney [7.5'] quadrangles, Oregon: Oregon Department of Geology and Mineral Industries Geologic Map Series GMS-18, 2 plates. **(9)**

Black, G. L., Woller, N. M., and Ferns, M. L., 1987, Geologic map of the Crescent Mountain area, Linn County, Oregon: Oregon Department of Geology and Mineral Industries Geologic Map Series GMS-47, 1 plate. **(16)**

Black, G. L., Wang, Z., Wiley, T., Keefer, D., and Wang, Y., 2000, Relative earthquake hazard map of the Eugene-Springfield metropolitan area, Lane County, Oregon: Oregon Department of Geology and Mineral Industries Interpretive Map Series IMS-14, 16 p., 1 plate. **(44)**

Brown, D. E., 1980, Preliminary geology and geothermal resource potential of the Belknap-Foley area, Oregon: Oregon Department of Geology and Mineral Industries Open-File Report O-80-2, 58 p., 1 plate. **(24)**

Brown, D. E., McLean, G. D., Woller, N. M., and Black, G. L., 1980, Preliminary geology and geothermal resource potential of the Willamette Pass area, Oregon: Oregon Department of Geology and Mineral Industries Open-File Report O-80-3, 65 p., 1 plate. **(21)**

Brownfield, M. E., 1982a, Geologic map of the Sheridan quadrangle, Polk and Yamhill Counties, Oregon: Oregon Department of Geology and Mineral Industries Geologic Map Series GMS-23, 1 plate. **(10)**

Brownfield, M. E., 1982b, Geologic map of the Grande Ronde quadrangle, Polk and Yamhill Counties, Oregon: Oregon Department of Geology and Mineral Industries Geologic Map Series GMS-24, 1 plate. **(11)**

Brownfield, M. E., 1982c, Preliminary geologic map of the Ballston quadrangle, Oregon: Oregon Department of Geology and Mineral Industries Open-File Report O-82-2, 1 plate. **(20)**

Brownfield, M. E., and Schlicker, H. G., 1981a, Preliminary geologic map of the Amity and Mission Bottom quadrangles, Oregon: Oregon Department of Geology and Mineral Industries Open-File Report O-81-5, 1 plate. **(22)**

Brownfield, M. E., and Schlicker, H. G., 1981b, Preliminary geologic map of the McMinnville and Dayton quadrangles, Oregon: Oregon Department of Geology and Mineral Industries Open-File Report O-81-6, 1 plate. **(23)**

Burns, S., Growney, L., Broderson, B., Yeats, R. S., and Popowski, T. A., 1997, Map showing faults, bedrock geology, and sediment thickness of the western half of the Oregon City 1:100,000 quadrangle, Washington, Multnomah, Clackamas, and Marion Counties, Oregon: Oregon Department of Geology and Mineral Industries Interpretive Map Series IMS-4, 1 plate. **(19)**

Burns, S. F., Burns, W. J., James, D. H., and Hinkle, J. C., 1998, Landslides in the Portland, Oregon, metropolitan area resulting from the storm of February 1996: Inventory map, database, and evaluation: Portland State University, Department of Geology, report to Metro, contract 905828, 68 p.

Burns, W. J., 1999, Engineering geology and relative stability of the southern half of Newell Creek Canyon, Oregon City, Oregon: Portland State University, Department of Geology, master's thesis, 143 p., 3 plates.

Cascadia Region Earthquake Workgroup (CREW), 2003, HAZUS scenario for a Cascadia Subduction Zone earthquake. Available on CD-ROM from CREW, c/o Bob Freitag, Executive Director, 3110 Portage Bay Pl E Slip G, Seattle, WA 98102. (http://www.crew.org/)

City of Ashland, 2005, Hosler dam failure study: Inundation path and FEMA floodplain map: City of Ashland website. (http://www.ashland.or.us/Files/inundate_sm.pdf.)

Clague, J. J., Atwater, B., Wang, K., Wang, Y., and Wong, I., 2000, Penrose Conference 2000, Great Cascadia Earthquake Tricentennial, program summary and abstracts: Oregon Department of Geology and Mineral Industries Special Paper 33, 156 p.

Day, R. W., 2002, Geotechnical earthquake engineering handbook: New York, McGraw-Hill, 700 p.

DigitalGlobe, 2004, Banda Aceh shore, Indonesia, before and after photos, 2004, web page. (http://homepage.mac.com/demark/tsunami/2.html) created by Tony Demark, images copyright DigitalGlobe (http://www.digitalglobe.com/).

Federal Emergency Management Agency (FEMA), 1996, February 1996 flooding, landslides, and stream erosion in the State of Oregon: Bothell, Wash., FEMA Region 10 Interagency Hazard Mitigation Team Report DR-1099-OR, 87 p.

Federal Emergency Management Agency (FEMA), 1999, HAZUS, FEMA's tool for estimating potential losses from natural disasters: Washington, D. C. (Also available on CD-ROM disks from FEMA: http://www.fema.gov/library/viewRecord.do?id=1753.)

Federal Emergency Management Agency (FEMA), 2003a, NEHRP recommended provisions for seismic regulations for new buildings and other structures, 2003 edition, FEMA publication 450: Washington, D. C., Building Seismic Safety Council, 365 p. (http://www.fema.gov/library/viewRecord.do?id=2020)

Federal Emergency Management Agency (FEMA), 2003b, HAZUS-MH, FEMA's tool for estimating potential losses from natural disasters: Washington, D. C., National Institute of Building Sciences. (Also available on CD-ROM from FEMA: http://www.fema.gov/plan/prevent/hazus/hz_orderform.shtm.)

Geomatrix Consultants, Inc., 1995, Seismic design mapping, State of Oregon; project no. 2442, prepared for Oregon Department of Transportation, personal services contract 11688: San Francisco, Calif., 252 p., 5 plates.

Goettel, K., and the Eugene-Springfield Emergency Management Team, 2004, Multihazard mitigation plan for Eugene-Springfield metropolitan area. (http://www.eugene-or.gov/portal/server.pt?open=512&objID=726&PageID=3695&cached=true&mode=2&userID=2)

Harvey, A., and Peterson, G., 1998, Water-induced landslide hazards, western portion of the Salem

Hills, Marion County, Oregon: Oregon Department of Geology and Mineral Industries Interpretive Map Series IMS-6, 13 p., 1 plate. **(51)**

Harvey, A., and Peterson, G., 2000, Water-induced landslide hazards, eastern portion of the Eola Hills, Polk County, Oregon: Oregon Department of Geology and Mineral Industries Interpretive Map Series IMS-5, 18 p., 1 plate. **(50)**

Hausler, E., and Sitar, N., 2001, Performance of soil improvement techniques in earthquakes: Berkeley, Pacific Earthquake Engineering Research Center, University of California. (http://library.eerc.berkeley.edu/archives/hausler/)

Hladky, F. R., and McCaslin, G. R., 2005, Preliminary geologic map of the Springfield quadrangle, Lane County, Oregon: Oregon Department of Geology and Mineral Industries Open-File Report O-06-07, 31 p., 1 plate. **(55)**

Hofmeister, R. J., 2000, Slope failures in Oregon: GIS inventory for three 1996/97 storm events: Oregon Department of Geology and Mineral Industries Special Paper 34, 20 p., 1 CD-ROM.

Hofmeister, R. J., and Wang, Y., 2000, Earthquake-induced slope instability: Relative hazard map, eastern portion of the Eola Hills, Polk County, Oregon: Oregon Department of Geology and Mineral Industries Interpretive Map Series IMS-18, 1 plate. **(49)**

Hofmeister, R. J., Wang, Y., and Keefer, D. K., 2000, Earthquake-induced slope instability: Relative hazard map, western portion of the Salem Hills, Marion County, Oregon: Oregon Department of Geology and Mineral Industries Interpretive Map Series IMS-17, 1 plate. **(48)**

Hofmeister, R. J., Miller, D. J., Mills, K. A., Hinkle, J. C., and Beier, A. E., 2002, GIS overview map of potential rapidly moving landslide hazards in western Oregon: Oregon Department of Geology and Mineral Industries Interpretive Map Series IMS-22, 52 p., 1 CD-ROM.

Holzer, T. H., 1994, Loma Prieta damage largely attributed to enhanced ground shaking: EOS, Transactions, American Geophysical Union, v. 75, no. 26, p. 299–301. [Reprinted in Oregon Geology, 1994, v. 56, no. 5, p. 111–113.]

Kanamori, H., 1977, The energy release in great earthquakes: Journal of Geophysical Research, v. 82, p. 2981–2987.

Kramer, S. L., 1996, Geotechnical earthquake engineering: Prentice Hall, New Jersey, 653 p.

Madin, I. P., and Murray, R. B., 2003, Preliminary geologic map of the Eugene East and Eugene West quadrangles, Lane County, Oregon: Oregon Department of Geology and Mineral Industries Open-File Report O-06-17, 20 p., 1 plate. **(56)**

Madin, I. P., and Murray, R. B., 2005, Preliminary geologic map of the Veneta quadrangle, Lane County, Oregon: Oregon Department of Geology and Mineral Industries Open-File Report O-06-13, 12 p., 1 plate. **(54)**

Madin, I. P., and Wang, Z., 1999, Relative earthquake hazard maps for selected coastal communities in Oregon: Astoria–Warrenton, Brookings, Coquille, Florence–Dunes City, Lincoln City, Newport, Reedsport–Winchester Bay, Seaside–Gearhart–Cannon Beach, and Tillamook: Oregon Department of Geology and Mineral Industries Interpretive Map Series IMS-10, 25 p., 36 plates. **(38)**

Madin, I. P., and Wang, Z., 2000a, Relative earthquake hazard maps for selected urban areas in western Oregon: Canby–Barlow–Aurora, Woodburn–Hubbard, Silverton–Mt. Angel, Stayton–Sublimity–Aumsville, Lebanon, Sweet Home: Oregon Department of Geology and Mineral Industries Interpretive Map Series IMS-8, 22 p., 24 plates. **(46, 47, 57, 58, 59, 60)**

Madin, I. P., and Wang, Z., 2000b, Relative earthquake hazard maps for selected urban areas in western Oregon: Ashland, Cottage Grove, Grants Pass, Roseburg, Sutherlin–Oakland: Oregon Department of Geology and Mineral Industries Interpretive Map Series IMS-9, 21 p., 20 plates. **(37)**

Madin, I. P., and Wang, Z., 2000c, Relative earthquake hazard maps for selected urban areas in western Oregon: St. Helens–Columbia City–Scappoose,

Sandy, Hood River, McMinnville–Dayton–Lafayette, Newburg–Dundee, Sheridan–Willamina, Dallas, Monmouth–Independence: Oregon Department of Geology and Mineral Industries Interpretive Map Series IMS-7, 24 p., 32 plates. **(39, 40, 41, 42, 43)**

Madin, I. P., Priest, G. R., Mabey, M. A., Malone, S., Yelin, T., and Meier, D., 1993, March 23, 1993, Scotts Mills earth-quake — western Oregon's wake-up call: Oregon Geology, v. 55, no. 3, p. 51–57.

Madin, I. P., Murray, R. B., and Hladky, F. R., 2006, Preliminary geologic map of the Coburg quadrangle, Lane and Linn Counties, Oregon: Oregon Department of Geology and Mineral Industries Open-File Report O-06-06, 24 p., 2 plates. **(55)**

Miller, P. R., and Orr, W. N., 1984a, Geologic map of the Wilhoit quadrangle, Oregon: Oregon Department of Geology and Mineral Industries Geological Map Series GMS-32, 1 plate. **(12)**

Miller, P. R., and Orr, W. N., 1984b, Geologic map of the Scotts Mills quadrangle, Oregon: Oregon Department of Geology and Mineral Industries Geological Map Series GMS-33, 1 plate. **(13)**

Murray, R. B., 2005, Preliminary geologic map of the Creswell quadrangle, Lane County, Oregon: Oregon Department of Geology and Mineral Industries Open-File Report O-06-12, 15 p., 1 plate. **(54)**

Nakata, J. K., and Peterson, D. M., 1990, Photographs of the October 17th 1989 Loma Prieta, California, earthquake: U.S. Geological Survey Open-File Report 90-547.

National Research Council (Commission on Engineering and Technical Systems, Committee on Earthquake Engineering), 1985, Liquefaction of soils during earthquakes: Washington, D.C., National Academy Press, 240 p.

Niem, A. R., Niem, W. A., and Baldwin, E. M., 1989, Geology and oil, gas, and coal resources of the southern Tyee Basin, southern Coast Range, Oregon: Oregon Department of Geology and Mineral Industries Open-File Report O-89-3, 44 p., 3 plates. **(26)**

Niewendorp, C. A., and Neuhaus, M. E., 2003, Map of selected earthquakes for Oregon, 1841 through 2002: Oregon Department of Geology and Mineral Industries Open-File Report O-03-02, 1 plate.

Nisqually Earthquake Information Clearinghouse, 2001. (http://www.ce.washington.edu/~nisqually/)

NW Geoscience.com, 2002, Resources relating to the Kelso, WA slide and slides in general, web page. (http://www.nwgeoscience.com/kelso/)

O'Connor, J., Sarna-Wojcicki, A., Wozniak, K. C., Polette, D. J., and Fleck, R. J., 2001, Origin, extent, and thickness of Quaternary geologic units in the Willamette Valley, Oregon: U.S. Geological Survey Professional Paper PP-1620, 52 p., 1 plate. **(52)**

Orr, W. N., and Miller, P. R., 1984, Geologic map of the Stayton NE quadrangle, Oregon: Oregon Department of Geology and Mineral Industries Geological Map Series GMS-34, 1 plate. **(14)**

Orr, W. N., and Miller, P. R., 1986, Geologic map of the Elk Prairie quadrangle, Marion and Clackamas Counties, Oregon: Oregon Department of Geology and Mineral Industries Geological Map Series GMS-51, 1 plate. **(18)**

Park, J., Anderson, K., Aster, R., Butler, R., Lay, T., and Simpson, D., 2005, Global seismic network records the great Sumatra-Andaman earthquake: EOS, Transactions, American Geophysical Union, v. 86, no. 6, p. 57–64.

Priest, G. R., 1995, Explanation of mapping methods and use of the tsunami hazard map of the Siletz Bay area, Lincoln County, Oregon: Oregon Department of Geology and Mineral Industries Open-File Report O-95-05, 69 p.

Priest, G. R., Woller, N. M., and Ferns, M. L., 1987, Geology of the Breitenbush River area, Linn and Marion Counties, Oregon: Oregon Department of Geology and Mineral Industries Geological Map Series GMS-46, 4 p., 1 plate. **(15)**

Priest, G. R., Black, G. L., Woller, N. M., and Taylor, E. M., 1988, Geologic map of the McKenzie Bridge [15′] quadrangle, Lane County: Oregon Department of Geology and Mineral Industries Geological Map Series GMS-48, 2 plates. **(17)**

Ramp, L., 1972, Geology and mineral resources of Douglas County, Oregon: Oregon Department

of Geology and Mineral Industries Bulletin B-75, 106 p., 1 plate. **(5)**

Ritter, D. F., Kochel, R. C., and Miller, J. R., 1995, Process geomorphology: Dubuque, Iowa, Wm. C. Brown Publishers, 546 p.

Rogers, A.M., Walsh, T. J., Kockelman, W. J., and Priest, G. R., eds., 1998, Assessing earthquake hazards and reducing risk in the Pacific Northwest, volume 2: U.S. Geological Survey Professional Paper 1560, 545 p.

Schlicker, H., and Deacon, R. J., 1967, Engineering geology of the Tualatin Valley region, Oregon: Oregon Department of Geology and Mineral Industries Bulletin B-60, 103 p., 4 plates. **(4)**

Schlicker, H., Deacon, R. J., Newcomb, R. C., and Jackson, R. L., 1974, Environmental geology of coastal Lane County, Oregon: Oregon Department of Geology and Mineral Industries Bulletin B-85, 116 p., 3 plates. **(7)**

Schuster, R. L., and Fleming, R. W., 1986, Economic losses and fatalities due to landslides: Bulletin of the Association of Engineering Geologists, v. 23, no. 1, p. 11–28.

Scott, W. E., Iverson, R. M., Schilling, S. P., and Fisher, B. J., 1999, Volcano hazards in the Three Sisters region, Oregon: U.S. Geological Survey Open-File Report 99-437, 14 p., 1 plate. (http://geopubs.wr.usgs.gov/open-file/of99-437/)

Seed, H. B., Romo, M. P., Sun, J. I., Jaime, A., and Lysmer, J., 1988, The Mexico earthquake of September 19, 1985 — relationship between soil conditions and earthquake ground motions: Earthquake Spectra, v. 4, p. 687–729.

Senneset, K., 1996., Landslides/glissements de terrain, International Symposium on Landslides, 7th, Trondheim, Norway, June 17–21, 1996, Proceedings: A.A. Balkema, p. 337–380.

Sherrod, D. R., 1988, Geology and geothermal resources of the Breitenbush-Austin Hot Springs area, Clackamas and Marion Counties: Oregon Department of Geology and Mineral Industries Open-File Report O-88-5. **(25)**

Snavely, P. D., MacLeod, N. S., Wagner, H. C., and Rau, W. W., 1976, Geologic map of the Waldport and Tidewater quadrangles, Lincoln, Lane, and Benton Counties, Oregon: U.S. Geological Survey Miscellaneous Investigations Series Map I-866, 1 plate. **(28)**

Spangle Associates, 1998, Using earthquake hazard maps: A guide for local governments in the Portland Metropolitan Region: Oregon Department of Geology and Mineral Industries Open-File Report O-98-4, 45 p.

Thayer, T. P., 1939, Geology of the Salem Hills and North Santiam River Basin: Oregon Department of Geology and Mineral Industries Bulletin B-15, 40 p., 1 plate. **(1)**

Tolan, T., Beeson, M., and Wheeler, K. L., 1999, Geologic map of the Scotts Mills, Silverton, and Stayton Northeast 7.5 minute quadrangles, northwest Oregon; a digital database: U.S. Geological Survey Open-File Report 99-141. **(32)**

Turner, A. K., and Schuster, R. L., eds., 1996, Landslides: Investigation and mitigation: Transportation Research Board, National Research Council, Special Report 247, 673 p.

U.S. Army Corps of Engineers, 2005, National inventory of dams. (http://crunch.tec.army.mil/nid/webpages/nid.cfm)

U.S. Geological Survey, 2004, National elevation dataset (NED). (http://ned.usgs.gov/)

U.S. Geological Survey Earthquake Program, 2004a, 2005 earthquake and news headlines archive: Magnitude 9.1 off the west coast of northern Sumatra December 26, 2004. (http://earthquake.usgs.gov/eqcenter/eqinthenews/2004/usslav/)

U.S. Geological Survey Earthquake Program, 2004b, Quaternary fault and fold database for the Nation. Online Database. (http://earthquake.usgs.gov/qfaults/)

U.S. Geological Survey Earthquake Program, 2005, 2005 earthquake and news headlines archive: Magnitude 8.6 northern Sumatra, Indonesia March 28, 2005. (http://earthquake.usgs.gov/eqcenter/eqinthenews/2005/usweax/)

Vokes, E. E., Snavely, P. D., and Myers, D. A., 1951, Geology of the southern and southwestern border area of the Willamette Valley, Oregon: U.S. Geological Survey Oil and Gas Investigations Map OM-110, 1 plate. **(30)**

Walder, J. S., Gardner, C. A., Conrey, R. M., Schilling, S. P., and Fisher, B. J., 1999, Volcano hazards in the Three Sisters Region, Oregon: U.S. Geological Survey Open-File Report 99-24, 14 p., 2 plates. (http://geopubs.wr.usgs.gov/open-file/of99-24/)

Walker, G. W., and Duncan, R. A., 1989, Geologic map of the Salem 1° × 2° quadrangle, western Oregon: U.S. Geological Survey Miscellaneous Investigations Series Map I-1893, 1 plate. **(29)**

Walker, G. W., MacLeod, N. S., Miller, R. J., Raines, G. L., and Connors, K. A., 2002, Spatial digital database for the geologic map of Oregon: U.S. Geological Survey Open-File Report 03-67, 21 p., digital database. **(53)**

Wang, Y., 1998, Earthquake damage and loss estimate for Oregon: Oregon Department of Geology and Mineral Industries Open-File Report O-98-3, 10 p., 2 appendixes.

Wang, Y., and Clark, J. L., 1999, Earthquake damage in Oregon: Preliminary estimates of future earthquake losses: Oregon Department of Geology and Mineral Industries Special Paper SP-29, 59 p.

Wang, Y., and Leonard, W. J., 1996, Relative earthquake hazard maps of Salem East and Salem West quadrangles, Marion and Polk Counties: Oregon Department of Geology and Mineral Industries Geological Map Series GMS-105, 10 p., 4 plates. **(34)**

Wang, Y., Summers, R. D., and Hofmeister, R. J., 2002, Landslide loss estimation pilot project in Oregon: Oregon Department of Geology and Mineral Industries Open-File Report O-02-05, 23 p.

Wang, Z., Graham, G. B., and Madin, I. P., 2001, Preliminary earthquake hazard and risk assessment and water-induced landslide hazard in Benton County, Oregon: Oregon Department of Geology and Mineral Industries Open-File Report O-01-05, 89 p., GIS data files. **(45)**

Washington State Department of Ecology, Water Resources, 1991, Seminary Hill reservoir failure. (http://www.ecy.wa.gov/programs/wr/dams/seminary.html)

Wells, R. E., Niem, A. R., MacLeod, N. S., Snavely, Jr., P. D., and Niem, W. A.,1983, Preliminary geologic map of west half of Vancouver (Wa.-Ore.) 1° × 2° quadrangle, Oregon: Oregon Department of Geology and Mineral Industries Open-File Report O-83-06, 1 plate. **(35)**

White, C. M., 1980, Geology of the Breitenbush Hot Springs quadrangle, Oregon: Oregon Department of Geology and Mineral Industries Special Paper SP-9, 26 p., 1 plate. **(27)**

Wiley, T. J., Sherrod, D. R., Keefer, D. K., Qamar, A., Schuster, R. L., Dewey, J. W., Mabey, M. A., Black, G. L., and Wells, R. E., 1993, Klamath Falls Earthquake, September 20, 1993 — Including the strongest quake ever measured in Oregon: Oregon Geology, v. 55, no. 6, p. 127–134.

Wilson, R. C., and Keefer, D. K., 1985, Predicting areal limits of earthquake-induced landsliding, *in* Ziony, J. L., ed., Evaluating earthquake hazards in the Los Angeles region; an earth-science perspective: U.S. Geological Survey Professional Paper 1360, p. 316–345.

Windmiller, J., 2000, Cypress Street Viaduct: California's first double-decker freeway: The Highwayman's Road Reports. (http://home.pacbell.net/hywaymn/Cypress_Viaduct_Freeway.html)

Yamaguchi, D. K., Atwater, B. F., Bunker, D. E., Benson, B. E., and Reid, M. S., 1997, Tree-ring dating the 1700 Cascadia earthquake: Nature, v. 389, p. 922.

Youd, T. L., and Perkins, D. M., 1978, Mapping liquefaction-induced ground failure potential: Journal of the Geotechnical Engineering Division, American Society of Civil Engineers, v. 104, no. GT4, p. 433–446.